BJP BRITISH JOURNAL OF PHARMACOLOGY
BPS BRITISH PHARMACOLOGICAL SOCIETY

BJP British Journal of Pharmacology

DOI:10.1111/j.1476-5381.2010.00889.x
www.brjpharmacol.org

RESEARCH PAPER

GSK1562590, a slowly dissociating urotensin-II receptor antagonist, exhibits prolonged pharmacodynamic activity *ex vivo*

DJ Behm, NV Aiyar, AR Olzinski, JJ McAtee, MA Hilfiker, JW Dodson, SE Dowdell, GZ Wang, KB Goodman, CA Sehon, MR Harpel, RN Willette, MJ Neeb, CA Leach and SA Douglas

Metabolic Pathways Center of Excellence for Drug Discovery, GlaxoSmithKline, King of Prussia, PA, USA

Correspondence
DJ Behm (UW2523), Metabolic Pathways Center of Excellence for Drug Discovery, GlaxoSmithKline, PO Box 1539, 709 Swedeland Road, King of Prussia, PA 19406-0939, USA.
E-mail: david.j.behm@gsk.com

Keywords
urotensin-II; UT; GSK1562590; GSK1440115; antagonist; blood pressure; G-protein-coupled receptor; residence time; dissociation rate;biochemical efficiency

Received
18 February 2010
Revised
5 April 2010
Accepted
14 April 2010

BACKGROUND AND PURPOSE
Recently identified antagonists of the urotensin–II (U-II) receptor (UT) are of limited utility for investigating the (patho)physiological role of U-II due to poor potency and limited selectivity and/or intrinsic activity.

EXPERIMENTAL APPROACH
The pharmacological properties of two novel UT antagonists, GSK1440115 and GSK1562590, were compared using multiple bioassays.

KEY RESULTS
GSK1440115 (pK_i = 7.34–8.64 across species) and GSK1562590 (pK_i = 9.14–9.66 across species) are high affinity ligands of mammalian recombinant (mouse, rat, cat, monkey, human) and native (SJRH30 cells) UT. Both compounds exhibited >100-fold selectivity for UT versus 87 distinct mammalian GPCR, enzyme, ion channel and neurotransmitter uptake targets. GSK1440115 showed competitive antagonism at UT in arteries from all species tested (pA_2 = 5.59–7.71). In contrast, GSK1562590 was an insurmountable UT antagonist in rat, cat and hUT transgenic mouse arteries (pK_b = 8.93–10.12 across species), but a competitive antagonist in monkey arteries (pK_b = 8.87–8.93). Likewise, GSK1562590 inhibited the hU-II-induced systemic pressor response in anaesthetized cats at a dose 10-fold lower than that of GSK1440115. The antagonistic effects of GSK1440115, but not GSK1562590, could be reversed by washout in rat isolated aorta. In *ex vivo* studies, GSK1562590 inhibited hU-II-induced contraction of rat aorta for at least 24 h following dosing. Dissociation of GSK1562590 binding was considerably slower at rat than monkey UT.

CONCLUSIONS AND IMPLICATIONS
Whereas both GSK1440115 and GSK1562590 represent high-affinity/selective UT antagonists suitable for assessing the (patho)physiological role of U-II, only GSK1562590 exhibited sustained UT residence time and improved preclinical efficacy *in vivo*.

Abbreviations
BacMam, recombinant baculovirus in which the polyhedrin promoter has been replaced with a mammalian promoter; CHO cells, Chinese hamster ovary cells; DMSO, dimethylsulphoxide; DPBS, Dulbecco's phosphate-buffered saline; FLIPR, fluorescence imaging plate reader; GPCR, G-protein-coupled receptor; GSK1440115, 4′-[(1R)-1-[[(6,7-dichloro-3-oxo-2,3-dihydro-4H-1,4-benzoxazin-4-yl)acetyl](methyl)amino]-2-(4-morpholinyl)ethyl]-4-biphenylcarboxylic acid trifluoroacetate; GSK1562590, 4′-[(1R)-1-[[(6,7-dichloro-3-oxo-2,3-dihydro-4H-1,4-benzoxazin-4-

yl)acetyl](methyl)amino]-2-(1-pyrrolidinyl)ethyl]-3-biphenylcarboxamide hydrochloride; HEK293, human embryonic kidney cells; NKA, neurokinin A; SJRH30, human rhabdomyosarcoma cell line; SPA, scintillation proximity assay; U2OS, human osteosarcoma cell line; (h)U-II, (human) urotensin-II; (h)UT, (human) urotensin-II receptor; WGA, wheat germ agglutinin-coated

Introduction

Human urotensin-II (hU-II) is a cyclic undecapeptide hormone and endogenous ligand of the G-protein-coupled U-II receptor, UT (nomenclature follows Alexander *et al.*, 2009). Functionally, hU-II is among 'the most potent mammalian vasoconstrictors identified to date' (Ames *et al.*, 1999). In addition to its vasoconstrictor activity, hU-II also modulates cardiac contractility (Russell *et al.*, 2001; Gong *et al.*, 2004; Quaile *et al.*, 2009), cardiomyocyte hypertrophy and fibrosis (Tzanidis *et al.*, 2003; Johns *et al.*, 2004; Onan *et al.*, 2004; Liu *et al.*, 2009), natriuresis (Song *et al.*, 2003; Zhang *et al.*, 2003) and insulin release (Silvestre *et al.*, 2001), raising the possibility that the hU-II/UT system plays a significant role in cardiovascular, renal and metabolic diseases.

Over the past decade, development of non-peptide UT antagonists has allowed investigators to begin to delineate the (patho)physiological role of the hU-II/UT system (see Maryanoff and Kinney, 2010). The most advanced drug candidate is Actelion's Palosuran (ACT-058362; Clozel *et al.*, 2004) but phase 2b clinical trials were ceased in May 2005 due to lack of efficacy in diabetic nephropathy patients (http://www1.actelion.com/documents/publications/Milestones_Company.pdf; Clozel *et al.*, 2006). However, it was recently suggested that this disappointing outcome with Palosuran might be the result of attenuated antagonist potency in intact cells/tissues (Behm *et al.*, 2008) or masking of activity due to clinical co-administration with angiotensin II pathway blockers, as required for ethical reasons (Sidharta *et al.*, 2006; Sidharta *et al.*, 2009).

As the (patho)physiological significance of the hU-II/UT pathway remains ambiguous, the identification of UT antagonists with high selectivity and pan-species activity remains greatly desired. In addition, the association of commercially available drugs which exhibit slow receptor dissociation rates with improved clinical efficacies (see Swinney, 2004 and Copeland *et al.*, 2006 for review) has raised interest in identifying UT antagonists with increased residence time (period of time that antagonist occupies its receptor). While optimizing high-throughput screening hits, we identified two compounds, GSK1440115 and GSK1562590 (Figure 1), which exhibited differential characteristics consistent with rapidly and slowly reversible modes of action respectively. The present study aimed to detail the pharmacological characteristics of both compounds and to test whether or not receptor dissociation rates extrapolated to altered efficacy *in vitro*, *ex vivo* and *in vivo*. Although both compounds are high-affinity/selective UT antagonists suitable for interrogating the (patho)physi-

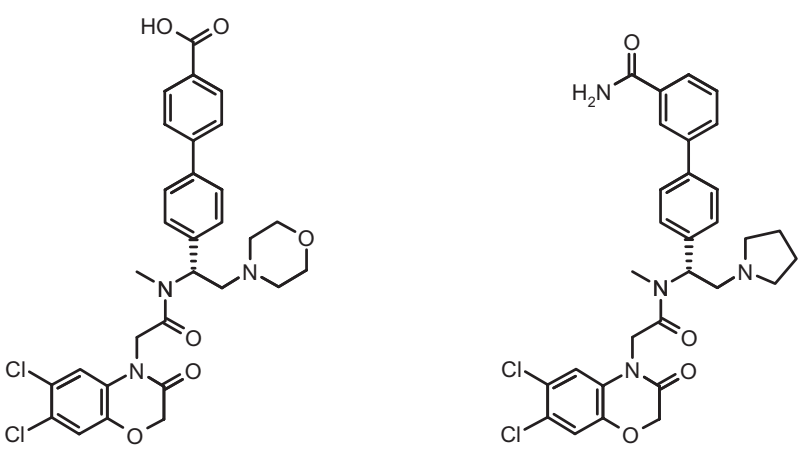

Figure 1

Structures of the novel UT antagonists (A) GSK1440115 (4′-[(1R)-1-[[(6,7-dichloro-3-oxo-2,3-dihydro-4H-1,4-benzoxazin-4-yl)acetyl](methyl)amino]-2-(4-morpholinyl)ethyl]-4-biphenylcarboxylic acid, trifluoroacetate) and (B) GSK1562590 (4′-[(1R)-1-[[(6,7-dichloro-3-oxo-2,3-dihydro-4H-1,4-benzoxazin-4-yl)acetyl](methyl)amino]-2-(1-pyrrolidinyl)ethyl]-3-biphenylcarboxamide, hydrochloride).

ological role of U-II, GSK1562590 represents the first UT antagonist with enhanced UT receptor residence time, resulting in extended duration of pharmacodynamic activity *ex vivo*.

Methods

All studies were performed in Association for Assessment and Accreditation of Laboratory Animal Care-accredited facilities in accordance with institutional guidelines.

Radioligand binding at recombinant UT

[^{125}I]hU-II competition binding assays were performed using membranes isolated from human osteosarcoma (U2OS) cells, transiently expressing rat or human UT, or human embryonic kidney (HEK293) cells, stably expressing mouse, cat or monkey UT (Ames *et al.*, 1999; Behm *et al.*, 2006). Following a 30 min incubation of membranes with polystyrene WGA-SPA beads (1:50, ww^{-1}) in assay buffer [20 mM Tris (pH 7.4) 5 mM $MgCl_2$ and 0.1% BSA] at room temperature, the bead : UT membrane mixture was combined with [^{125}I]hU-II (0.6 nM final concentration) and added to 384-well Proxy plates (Perkin Elmer, Shelton, CT) containing 0.1 nM–10 μM GSK1440115 or GSK1562590 or DMSO vehicle (1% final). Plates were incubated for 2 h (monkey and mouse UT) to 3 h (human, cat and rat UT) at room temperature and then read using scintillation counting (Viewlux or TopCount; Perkin Elmer). Non-specific binding was defined using 1 μM unlabelled hU-II.

Radioligand binding at native UT in human SJRH30 cells

Whole cell [^{125}I]hU-II competition binding assays were performed at native human UT using intact SJRH30 cells (human rhabdomyosarcoma cell line; Douglas *et al.*, 2004b). Assays were performed with 200 pM [^{125}I]hU-II in the presence or absence of 1 pM-1 μM unlabelled hU-II, GSK1440115 or GSK1562590 in Dulbecco's phosphate-buffered saline (DPBS$^+$; 0.7 mM $CaCl_2$, 10 mM $MgCl_2$, 1.4 mM glucose, 0.2% BSA). Assay plates were incubated at 37°C for 30 min. Following three washes with DPBS$^+$, the cells were lysed with 2N NaOH and the resulting lysate was counted using a gamma counter (Wallac Wizard™; Perkin Elmer). Non-specific binding was defined using 1 μM unlabelled hU-II.

Reversibility of ligand binding at rat, monkey and human UT

Rat, monkey and human UT membranes were incubated with DMSO or 10 nM GSK1562590 for 30 min at 25°C. Following this equilibration period, incubation mixtures were diluted in buffer [25 mM Tris-HCl (pH 7.4), 5 mM $MgCl_2$, 2 mM Na-EGTA, 0.1 mg·mL^{-1} bacitracin] and centrifuged (47 000× *g*, 20 min, 4°C). The membrane pellets were then resuspended in buffer following which [^{125}I]hU-II binding site density (B_{max}) and affinity (K_D) values were determined ($t = 0$). At $t = 0.5$, 1 or 2 h following the initial resuspension, a subset of membranes were 'washed' a second time and subjected to B_{max} and K_D determination. B_{max} and K_D values were determined by homologous competition binding (Wallac Wizard™) whereby multiple concentrations of unlabelled hU-II were used to compete for binding with a fixed concentration of [^{125}I]hU-II (Douglas *et al.*, 2005).

Secondary pharmacological profiling

The secondary pharmacological properties of 1 μM GSK1440115 and 1 μM GSK1562590 (concentrations >400- and 1900-fold above the human recombinant UT K_i values respectively) were initially characterized using a panel of 87 binding assays for distinct mammalian G-protein-coupled receptor, enzyme, ion channel and neurostransmitter uptake targets (Cerep, Paris, France): adenosine ($A_{1,2A,3}$), adrenoceptors (non-selective $\alpha_{1,2}$, $\alpha_{1A,1B,2B,2C}$, $\beta_{1,2,3}$), angiotensin ($AT_{1,2}$), central benzodiazepine (BZD), bradykinin (B_2), cannabinoid ($CB_{1,2}$), cholecystokinin (CCK_1), calcitonin gene-related peptide (CGRP), dopamine ($D_{1,2S,3,4.4}$), endothelin ($ET_{A,B}$), GABA (non-selective, $GABA_A$), AMPA, kainate, NMDA, galanin (Gal_2), Il-8 (CXCR2), histamine ($H_{1,2}$), imidazoline (I_2), leukotriene (BLT_1), melanocortin (MC_4), melatonin (MT_1), muscarinic ($M_{1\text{-}4}$), neuronal nicotinic, neuropeptide Y ($Y_{1,2}$), neurotensin (NTS_1), opioid (δ_2, κ, μ, σ), P_{2X}, 5-HT (5-$HT_{1A,1B,1D,2A,2C,3,4e,5A,6,7}$), tachykinin ($NK_{2,3}$), vasoactive intestinal peptide ($VPAC_1$), vasopressin (V_{1a}), oestrogen ($ER_{a,b}$), progesterone (PR) and androgen (AR) receptors, Ca^{2+} (L-type), K^+ (K_V, SK_{Ca}), Na^+ and Cl^- channels, and noradrenaline and dopamine transporters. All assays were performed using human orthologues except non-selective α, and α_{1A} adrenoceptors, σ opioid, AMPA, BZD, GABA, kainate, NMDA, I_2, P_{2X}, 5-HT_{1B}, Ca^{2+}, K_V, SK_{Ca}, Na^+, Cl^- (rat), κ opioid (guinea-pig) and 5-HT_{1D} (bovine) receptors. Dose–response curves were obtained for several of the more significant interactions (>50% activity) observed during the initial 1 μM screen.

Human κ opioid receptor (κ) agonism

κ opioid receptor agonism was measured using a [^{35}S]GTPγS binding assay for human κ opioid receptor (κ) stably expressed in hamster CHO

cell membranes. Assays were performed in the presence of DMSO vehicle (1%), GSK1440115 or GSK1562590, in a buffer containing 20 mM HEPES, 10 mM $MgCl_2$, 100 mM NaCl (adjusted to pH 7.4 with KOH) and 10 μM GDP. Incubations were performed for 3–5 h (room temperature) at which point [^{35}S]GTPγS SPA binding was evaluated using a Wallac 1430 ViewLux plus microplate imager.

Human tachykinin (hNK_2) receptor antagonism

Inhibition of EC_{80} neurokinin A (NKA)-mediated Ca^{2+}-mobilization was assessed using fluo-4-loaded, intact U2OS cells expressing human recombinant NK_2 receptor by FLIPR (fluorescence imaging plate reader; Molecular Devices, Sunnyvale, CA) analysis in the presence of DMSO vehicle (1%), GSK1440115 or GSK1562590. Assays were performed in HEPES buffered saline [20 mM HEPES, 145 mM NaCl, 5 mM KCl, 1 mM $CaCl_2$, 5.6 mM glucose (pH 7.3)].

Radioligand binding at NK_2, 5-HT_{1A} and D_{2S} receptors

[^{3}H]8-OH-DPAT and [^{3}H]spiperone competition binding assays were performed using HEK293 cell membranes stably expressing human recombinant 5-HT_{1A} and D_{2S} receptors respectively. The [^{125}I]NKA competition binding assay was performed using NK_2 BacMam transduced CHOK1 cells. Briefly, varying concentrations of GSK1562590 (10 nM–30 μM) were added to cell membranes in the presence of 3 nM [^{3}H]8-OH-DPAT, 3 nM [^{3}H]spiperone or 0.15 nM [^{125}I]NKA. Plates were incubated for 1 h at room temperature and SPA binding was determined via scintillation counting. Non-specific binding was defined using 10 μM 8-OH-DPAT (+)butaclamol or [Nle^{10}]-NKA (4–10).

Mammalian in vitro *vascular contractility assessment*

Proximal descending thoracic aortae were isolated from male Sprague-Dawley rats (400–500 g, Charles River, Raleigh, NC) and hUT transgenic mice (25–35 g; Behm *et al.*, 2008) following induction of anaesthesia (5% isoflurane in O_2) and exsanguination. Following sodium pentobarbitone overdose (100 mg·kg^{-1}, i.v.), mesenteric resistance arteries, femoral arteries and thoracic aortae were isolated from adult male cats (4–5 kg; Liberty Research Inc., Waverly, NY) and renal and superior mesenteric arteries were isolated from male cynomolgus monkeys (4–7 kg; Primate Products, Miami, FL; Covance, Alice TX; Charles River, Andover MA; Mannheimer, Homestead, FL).

Conduit arterial rings (approximately 3 mm in length) were denuded of endothelium by rubbing the lumen with a fine forceps and suspended in Krebs solution of the following composition (mM): NaCl (112.0), KCl (4.7), KH_2PO_4 (1.2), $MgSO_4$ (1.2), $CaCl_2$ (2.5), $NaHCO_3$ (25.0), dextrose (11.0), indomethacin (0.01). Isometric force responses were measured (MLT0201/D transducers; Letica, Barcelona, Spain) under optimal resting tension (1.0 g, 2.0 g, 2.0 g and 0.5 g in rat, cat, monkey and transgenic mouse vessels respectively; Douglas *et al.*, 2000; Behm *et al.*, 2004). Cat endothelium-intact mesenteric resistance arteries (125–150 μm internal diameter) were mounted on a wire myograph (Danish myotechnologies, Aarhus, Denmark) under 0.5 g optimal resting tension. Changes in isometric force were recorded digitally (ADInstruments Chart 5.0 software, Colorado Springs, CO, USA). Following 1 h equilibration, vessels were treated with 60 mM KCl and 1 μM phenylephrine (subsequent responses were normalized to KCl). Once the contractile response to phenylephrine reached a plateau, carbachol (10 μM) was added in order to evaluate functional endothelial integrity.

Arteries were pretreated (30 min) with vehicle (0.1% DMSO), GSK1440115 (300–10 000 nM) or GSK1562590 (0.001–1000 nM), following which cumulative concentrations of hU-II (0.01–10 000 nM) were added to the tissue baths at half-log increments. Contractile responses to each concentration of hU-II were allowed to reach a plateau (~10–15 min) before the addition of subsequent concentrations, and only one concentration–response curve was generated per tissue. In separate experiments, selectivity studies were performed with GSK1440115 (3 μM) and GSK1562590 (0.3 μM) using non-UT spasmogens (KCl, phenylephrine and endothelin-1).

Reversibility of UT antagonism in rat isolated aorta: in vitro *washout studies*

Cumulative concentration–response curves to hU-II (0.1 nM–3 μM) were generated following a 30 min pretreatment with vehicle (0.1% DMSO), GSK1440115 (1000 nM) or GSK1562590 (0.3 nM). Separate tissues were washed repeatedly for 1.5–24 h with fresh Krebs solution (not containing antagonist) before generating the hU-II concentration–response curves.

Reversibility of UT antagonism in rat isolated aorta: ex vivo *studies*

Male Sprague-Dawley rats (400–500 g) were dosed via oral gavage with vehicle (5% DMSO, 20% hydroxylpropyl-beta-cyclodextran) or GSK1562590

(1 mg·kg^{-1}). Following time periods ranging from 2–48 h, rats were anaesthetized with inhaled isoflurane (5% in O_2) and killed by cervical dislocation and exsanguination. Rings of the proximal descending thoracic aorta were suspended in tissue baths for generation of hU-II concentration–response curves (0.1 nM–10 μM) as described above. Blood was collected just before death for determining plasma drug concentrations.

Haemodynamic assessment in the anaesthetized cat

Haemodynamic measurements were made in anaesthetized cats as previously described (Behm *et al.*, 2004). Briefly, male and female cats (1–4 kg) were initially anaesthetized with ketamine (3 mg·kg^{-1}, i.m.) followed by isoflurane (5% in O_2) and artificially ventilated via a tracheal cannula (Model 665 ventilator, Harvard Apparatus, Holliston, MA). Femoral arteries were catheterized for the measurement of mean, systolic and diastolic arterial blood pressure. A Swan-Gantz catheter was inserted into the left femoral vein and advanced into the pulmonary artery to measure cardiac output by thermodilution (Cardiomax, Columbus, OH). A pressure transducer was advanced into the left ventricle via the carotid artery. A lead II ECG was also recorded via limb lead electrodes. Pressure, ECG and blood flow signals were pre-amplified (Astro-Medical, West Warwick, RI) prior to digitization (500 Hz) using a computerized data acquisition system (CA recorder, DISS, Integrated Telemetry Systems, Dexter, MI). ECG intervals were subsequently analysed using computerized pattern recognition analysis (Emka Technologies, Falls Church, VA). Following surgical instrumentation, anaesthesia was maintained with α-chloralose (65 mg·kg^{-1}, i.v. bolus) and haemodynamics and blood gases were allowed to stabilize (~20 min). At 60 min prior to hU-II administration (1 nmol·kg^{-1}, i.v. bolus), cats were pretreated with vehicle (5% DMSO, 20% aqueous Cavitron™ [hydroxypropyl-β-cyclodextrin]), GSK1440115 (0.3, 1, 3 and 10 mg·kg^{-1}) or GSK1562590 (0.01, 0.03, 0.1, 1 and 10 mg·kg^{-1}) via a 30 min i.v. infusion (0.167 mL·min^{-1}).

Quantification of plasma drug levels

Plasma levels of GSK1440115 and GSK1562590 were determined using liquid chromatography/tandem mass spectrometric (LC/MS/MS) detection. Briefly, drug levels were quantified via selected reaction monitoring of the transition from ionized drug (m/z = 598 and 582 for GSK1440115 and GSK1562590 respectively) to the fragment ion (m/z = 511 and 511 respectively) using atmospheric pressure chemical ionization on an Applied Biosystems API 5000 (Foster City, CA).

Data analysis

Unless stated otherwise, all values are mean ± standard error of the mean and n represents the total number of animals studied or individual experiments performed. Competition binding curves were analysed by non-linear regression (GraphPad Prism, La Jolla, CA) using the equation by Cheng & Prusoff (1973):

$$K_i = \frac{IC_{50}}{1+[A]/K_D}$$

where [A] represents the concentration of competing ligand (GSK1440115 or GSK1562590), IC_{50} the concentration of competing ligand that inhibits radiolabel binding by 50% and K_D the equilibrium dissociation constant of the radioligand.

Concentration-dependent contractility curves were fitted to a logistic equation as previously described (Douglas *et al.*, 2005):

$$E = \frac{E_{max}[C]^{n_H}}{EC_{50}^{n_H}+[C]^{n_H}}$$

where E is the contractile response, [C] the concentration of agonist, EC_{50} the concentration of agonist required to produce a half maximal response, n_H the Hill coefficient and E_{max} the maximum contractile response.

Empirical measurements of competitive antagonist potencies (pA_2, determined using a single concentration of antagonist) were calculated using the Schild equation (Jenkinson *et al.*, 1998):

$$pA_2 = \mathrm{Log}(DR-1) - \mathrm{Log}[B]$$

where DR is the dose-ratio (ratio of equiactive concentrations of agonist in the presence and absence of antagonist) and [B] is the concentration of antagonist.

Competitive antagonist affinities generated using multiple concentrations of antagonist [the equilibrium dissociation constant pK_b and associated 95% confidence intervals (CI)] were calculated using non-linear regression (Clark) analysis (Lew and Angus, 1997):

$$pEC_{50} = -\mathrm{Log}([B]+10^{-pK_b}) - \mathrm{Log}c$$

where [B] is the antagonist concentration and Log c is the difference between the antagonist pK_b and the agonist control curve pEC_{50}.

Noncompetitive antagonist affinities (pK_b) were determined using the method of Gaddum where equiactive concentrations of agonist in the absence

or presence of the noncompetitive antagonist were compared in a linear regression (Gaddum *et al.*, 1955; Kenakin, 2006). The resulting slope was used to calculate the equilibrium constant K_b using the following equation:

$$K_b = \frac{[B]}{(\text{slope} - 1)}$$

Where [B] is the antagonist concentration and slope is calculated from the double reciprocal plot of equiactive concentrations of agonist in the presence and absence of antagonist.

Areas under the blood pressure responses following hU-II administration were calculated by applying the trapezoid rule. Statistical comparisons were made using paired, two-tailed *t*-tests or ANOVA (with Dunnett's or Bonferroni multiple comparisons post-tests) and values were considered significantly different when $P \leq 0.05$.

Materials

GSK1440115 (4′-[(1R)-1-[[(6,7-dichloro-3-oxo-2,3-dihydro-4H-1,4-benzoxazin-4-yl)acetyl](methyl)amino]-2-(4-morpholinyl)ethyl]-4-biphenylcarboxylic acid, trifluoroacetate; Figure 1) and GSK1562590 (4′-[(1R)-1-[[(6,7-dichloro-3-oxo-2,3-dihydro-4H-1,4-benzoxazin-4-yl)acetyl](methyl)amino]-2-(1-pyrrolidinyl)ethyl]-3-biphenylcarboxamide, hydrochloride; Figure 1) were synthesized at GlaxoSmithKline (King of Prussia, PA). hU-II, [^{125}I] hU-II (Tyr^9 monoiodinated) and endothelin-1 were synthesized by California Peptide Research Inc. (Napa, CA), Perkin Elmer (Shelton, CT) and American Peptide Company, Inc. (Sunnyvale, CA) respectively. Leadseeker WGA-SPA beads were from Amersham (Arlington, Heights, IL). Isoflurane, ketamine and sodium pentobarbital were from Abbott Laboratories (North Chicago, IL), Fort Dodge Animal Health (Ford Dodge, IA) and Vortech Pharmaceuticals (Dearborn, MI) respectively. α-chloralose (Spectrum Chemical, New Brunswick, NJ) was freshly prepared as a sterile saline solution (40 mg·mL^{-1}) containing 25 mg·mL^{-1} of sodium bicarbonate (JT Baker, Phillipsburg, NJ) and 20 mg·mL^{-1} sodium tetraborate decahydrate (Sigma, St. Louis, MO). Carbachol, indomethacin, phenylephrine were from Sigma. All other reagents were of analytical grade.

Results

Radioligand binding at recombinant UT

GSK1440115 (pK_i = 7.34–8.64) and GSK1562590 (pK_i = 9.14–9.66) functioned as high affinity ligands at all recombinant mammalian UT orthologues studied, including mouse, rat, cat, monkey and human. Overall, GSK1562590 was a 5- to 101-fold more potent ligand across species as compared with GSK1440115. Hill slopes approximated unity for GSK1440115 and GSK1562590 (ranging from 0.70 to 0.94 and 0.95 to 1.47 respectively), indicating non-cooperative interactions with a single class of binding sites (Table 1). Both compounds consistently displaced the radioligand [^{125}I]hU-II by 100%.

Radioligand binding at native UT in human SJRH30 cells

In accordance with the pK_i values determined for human recombinant UT, both GSK1440115 and GSK1562590 potently inhibited [^{125}I]hU-II binding to endogenously expressed human UT in intact SJRH30 cells. Similar to the fivefold difference observed at the recombinant receptor, GSK1562590 was 15-fold more potent than GSK1440115 (pK_i values of 9.46 ± 0.06 and 8.38 ± 0.11 respectively; n = 4) (Table 1).

Table 1

GSK1440115 and GSK1562590 binding affinities to recombinant and native mammalian UT

UT orthologue	pK_i GSK1440115	GSK1562590	n_H GSK1440115	GSK1562590	*n* GSK1440115	GSK1562590	Relative affinity
Mouse (recombinant)	7.34 ± 0.07	9.34 ± 0.02	0.93 ± 0.04	1.47 ± 0.05	4	13	101-fold
Rat (recombinant)	8.49 ± 0.25	9.66 ± 0.04*	0.70 ± 0.09	0.95 ± 0.05	4	10	25-fold
Cat (recombinant)	8.45 ± 0.15	9.64 ± 0.03†	0.78 ± 0.05	1.39 ± 0.03	4	13	22-fold
Monkey (recombinant)	7.53 ± 0.12	9.14 ± 0.03	0.94 ± 0.05	1.05 ± 0.03	4	13	48-fold
Human (recombinant)	8.64 ± 0.06	9.28 ± 0.0†	0.88 ± 0.02	1.07 ± 0.02	12	33	5-fold
Human (native; SJRH30)	8.38 ± 0.11	9.46 ± 0.06	0.81 ± 0.08	1.09 ± 0.15	4	4	15-fold

*pK_i > 9.79 observed in n = 5 additional experiments.
†pK_i > 9.79 observed in n = 2 additional experiments.
GSK1440155 and GSK1562590 consistently displaced the radioligand [^{125}I]hU-II by 100%. All values are expressed as mean ± SEM.

Table 2

Secondary *in vitro* pharmacological properties of GSK1440115 and GSK1562590 (% inhibition of radioligand binding at 1 μM)

Target	Species	Radioligand	% inhibition at 1 μM GSK1440115	GSK1562590
κ opioid	guinea-pig	[^{3}H]U-69593	99	100
NK_2	human	[^{125}I]NKA	29	81
$GABA_A$	rat	[^{3}H]muscimol	27	<20
5-HT_{1A}	human	[^{3}H]8-OH-DPAT	22	90
5-HT_{2A}	human	[^{3}H]ketanserin	21	22
μ opioid	human	[^{3}H]DAMGO	20	49
D_{2S}	human	[^{3}H]spiperone	<20	82
α_{2C}	human	[^{3}H]RX821002	<20	50
α_{1A}	rat	[^{3}H]prazosin	<20	47
α_{1B}	human	[^{3}H]prazosin	<20	44
DA transporter	human	[^{3}H]BTCP	<20	38
α_1 (non-selective)	rat	[^{3}H]prazosin	<20	36
M_3	human	[^{3}H]4-DAMP	<20	29
NE transporter	human	[^{3}H]nisoxetine	<20	22
M_2	human	AF-DX 384	<20	20
δ opioid	human	[^{3}H]DADLE	<20	20
All other targets	–	–	<20	<20

All values are expressed as mean (n = 2).
5-$HT_{1A/2A}$, 5-hydroxytryptamine receptors; $\alpha_{1/1A/1B/2C}$, α-adrenoceptors, D_{2S}, dopamine receptor; DA transporter, dopamine transporter; $GABA_A$, gamma-aminobutyric acid receptor; $M_{2/3}$, muscarinic receptors; NE transporter, noradrenaline transporter; NK_2, tachykinin B receptor.

Table 3

Secondary *in vitro* pharmacological properties of GSK1440115 and GSK1562590 (potency determination)

Recombinant human receptor target	Potency GSK1440115	GSK1562590	Selectivity relative to human UT pK_i GSK1440115	GSK1562590
D_{2S} (pK_i)	–	7.02 ± 0.03 (n = 3)	–	194
κ opioid (pEC_{50})	5.63 ± 0.27 (n = 7)	6.94 ± 0.05 (n = 9)	2113	242
5-HT_{1A} (pK_i)	–	6.83 ± 0.03 (n = 3)	–	444
NK_2 (pK_i)	–	5.71 ± 0.25 (n = 2)	–	356
NK_2 (pK_b)	5.31 ± 0.04 (n = 2)	5.65 ± 0.08 (n = 2)	1988	4596

GSK1440115 and GSK1562590 did not antagonize the κ opioid receptor (pK_b < 5.12). Relative affinities/activities for GSK1440115 and GSK1562590 are expressed relative to their respective human UT pK_i values. All values are expressed as mean ± SEM.

Secondary pharmacology profiling

The only 'non-UT' assay in which >30% inhibition was observed with 1 μM GSK1440115 was at the κ opioid receptor (99% inhibition of [^{3}H]U-69593 binding in guinea-pig cerebellum; Table 2). In accord with these observations, GSK1440115 was a full agonist of the human κ opioid receptor (κ), providing an pEC_{50} of 5.63 ± 0.27 (>1000-fold selectivity relative to human UT pK_i value; Table 3) in an [^{35}S]GTPγS binding assay.

The initial selectivity profile of 1 μM GSK1562590 suggested appreciable interactions (>30% inhibition) with aminergic receptors (5-HT, dopamine, α-adrenoceptors), peptidergic receptors (opioid, tachykinin) and the dopamine transporter (Table 2). Less than 30% inhibition was seen in all other assays tested. Several of the more significant interactions (>50% inhibition at 1 μM) were profiled in more detail. Accordingly, GSK1562590 functioned as a ligand for 5-HT_{1A} and D_{2S} receptors, and

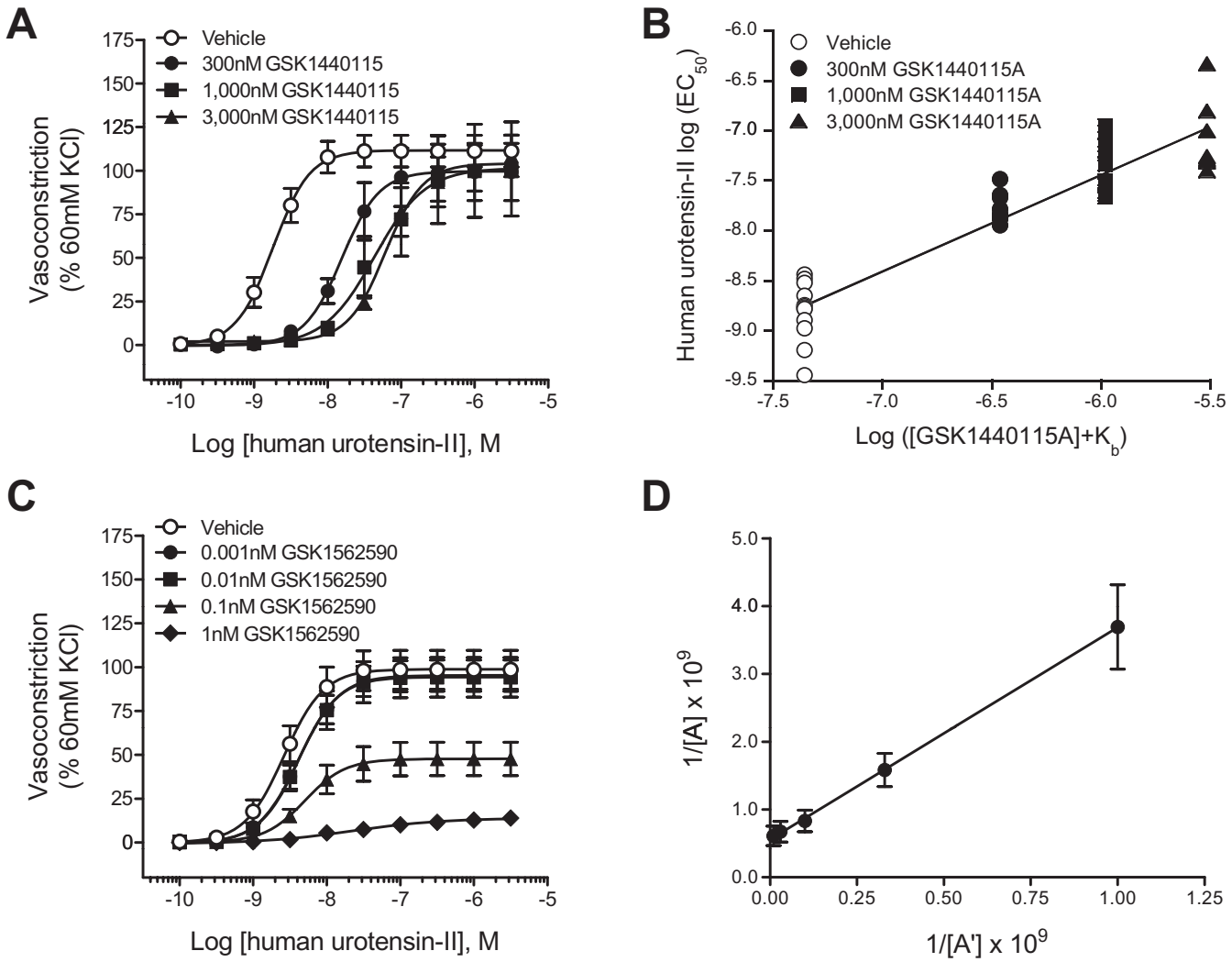

Figure 2

Inhibition of hU-II-induced contraction of rat isolated aortae by GSK1440115 and GSK1562590. (A) GSK1440115 elicited parallel, rightward shifts in the hU-II concentration–response curve. (B) Clark plot (global nonlinear regression analysis) revealed pA_2 = 7.36 (7.18–7.54 95% CI) and n_H = 0.97 (0.84–1.09 CI) consistent with competitive hU-II antagonism. In contrast to GSK1440115 (C) GSK1562590 suppressed the maximum contractile response to hU-II in a concentration-dependent manner (half-log unit values of GSK1562590 were removed for ease of interpretation). (D) Double reciprocal plot of equiactive concentrations of hU-II in the absence (A) and presence (A') of 0.1 nM GSK1562590 is linear (consistent with noncompetitive antagonism) with a slope of 3.13 ± 0.51, indicating a pK_b of 10.21 ± 0.11.

as a κ opioid receptor agonist and a NK_2 antagonist (Table 3), but still with ≥194-fold selectivity for the human UT (0.5 nM UT pK_i).

Functional potency in rat isolated aortae

GSK1440115 (0.3–3.0 μM) antagonized hU-II-induced contraction of the rat aorta in a concentration-dependent manner with a pK_b of 7.36 (7.18–7.54 95% CI; Figure 2A–B, Table 4). Clark analysis was consistent with a competitive, surmountable mode of action [n_H = 0.97 (0.84–1.09 95% CI)].

In contrast to GSK1440115, which functioned as a competitive hU-II antagonist, GSK1562590 suppressed the maximum contractile response to hU-II (Figure 2C; Table 4). Consistent with non-competitive antagonism, the slope of the double reciprocal plot of equiactive concentrations of agonist in the presence and absence of 0.1 nM GSK1562590 was linear with a slope of 3.13 ± 0.51, equating to a pK_b of 10.21 ± 0.11 (Figure 2D). As such, GSK1562590 was >2-orders of magnitude more potent as a UT antagonist in the rat isolated aorta than GSK1440115.

Table 4

Concentration-dependent inhibition of hU-II-induced contraction of rat isolated aorta by GSK1440115 and GSK1562590

GSK1440115 (nM)	hU-II E_{max} (% KCl)	hU-II pEC_{50}	Dose-ratio
Vehicle (n = 13)	111 ± 9	8.80 ± 0.08	–
300 (n = 8)	100 ± 17	7.76 ± 0.05***	10.2 ± 1.9
1000 (n = 12)	100 ± 26	7.37 ± 0.07***	30.9 ± 5.2
3000 (n = 8)	110 ± 12	7.09 ± 0.13***	52.7 ± 13.3
GSK1562590 (nM)	**hU-II E_{max} (% KCl)**	**hU-II pEC_{50}**	**Dose-ratio**
Vehicle (n = 11)	98 ± 11	8.55 ± 0.07	–
0.001 (n = 10)	95 ± 9	8.38 ± 0.06	1.8 ± 0.3
0.003 (n = 10)	74 ± 11	8.19 ± 0.12	4.1 ± 1.5
0.01 (n = 11)	94 ± 11	8.35 ± 0.05	1.7 ± 0.2
0.03 (n = 10)	70 ± 11	8.46 ± 0.06	1.4 ± 0.2
0.1 (n = 10)	48 ± 10**	8.29 ± 0.02	2.1 ± 0.4
0.3 (n = 10)	38 ± 9**	7.93 ± 0.07***	6.0 ± 1.9
1 (n = 10)	14 ± 2**	7.51 ± 0.17***	22.6 ± 8.5

All values are expressed as mean ± SEM. Statistical comparisons for both pEC_{50} and E_{max} values were performed using ANOVA analysis with a Dunnett's post-test where $^{**}P < 0.01$ and $^{***}P < 0.001$ versus vehicle control values. Global nonlinear regression (Clark) analysis of the competitive UT antagonist GSK1440115 resulted in a pA_2 of 7.36 (7.18–7.54 95% CI; Figure 2A–B). Linear regression analysis of 0.1 nM GSK1562590 using the method of Gaddum resulted in a linear plot (consistent with competitive antagonist) with a slope of 3.13 ± 0.51, equating to a pK_b of 10.21 ± 0.11 (Figure 2D).

Pretreatment of rat isolated aorta with either GSK1440115 or GSK1562590 did not alter basal contractile tone. Similarly, both compounds were devoid of intrinsic contractile activity in all other tissues/species studied.

Functional potency in cat isolated arteries

GSK1440115 (1 and 10 μM) antagonized hU-II-induced contraction in cat isolated conduit arteries (femoral artery and thoracic aorta) in a competitive manner (surmountable inhibition with no suppression of E_{max}; Figure 3A,C; Table 5). Similarly, competitive antagonism was also evident with GSK1440115 (1 μM) in cat mesenteric resistance arteries (Figure 3E; Table 5).

Consistent with data generated in rat aortae, GSK1562590 suppressed the maximal contractile response to hU-II in cat isolated arteries (Figure 3B,D,F; Table 6). Noncompetitive antagonist affinity values (pK_b) determined via the method of Gaddum indicated GSK1562590 was >two orders of magnitude more potent in cat isolated conduit arteries than GSK1440115 (Figure 3B,D,F; Table 6).

Functional potency in monkey isolated arteries

GSK1440115 (10 μM) antagonized hU-II-induced contraction in monkey renal and superior mesenteric arteries in a competitive manner (no suppression of E_{max}; Figure 4A,C; Table 5). As observed in cat isolated conduit vessels, the affinity of GSK1440115 in monkey conduit arteries (pA_2 = 6.46–6.63) is 6- to 18-fold lower than those observed in smaller diameter vessels such as the rat aortae (pK_b = 7.36) and cat mesenteric resistance vessels (pA_2 = 7.71).

In contrast to rat and cat arteries where GSK1562590 suppressed the maximum contractile response to hU-II, GSK1562590 acted as a competitive UT antagonist in monkey isolated arteries (Figure 4B,D; Table 6). Global non-linear regression (Clark) analysis revealed pK_b values of 8.93 (8.47–9.39 95% CI) and 8.87 (8.32–9.43 95% CI) for GSK1562590 in monkey isolated renal and superior mesenteric arteries [slopes of 0.89 (0.73–1.05 95% CI) and 0.96 (0.75–1.17 95% CI) and E_{max} unaltered, consistent with a competitive mode of antagonism; Figure 4E–F]. As such, GSK1562590 was >235-fold more potent in monkey isolated arteries than GSK1440115.

Functional potency in hUT transgenic mouse isolated aortae

GSK1440115 (10 μM) competitively inhibited (*i.e.* surmountable inhibition with no E_{max} suppression) hU-II-induced contraction of aortae isolated from transgenic mice expressing the human UT with a pA_2 of 7.41 ± 0.06 (Figure 5A; Table 5).

GSK1562590 (3 nM) functioned as a non-competitive antagonist in the hUT transgenic mouse isolated aorta, completely ablating the

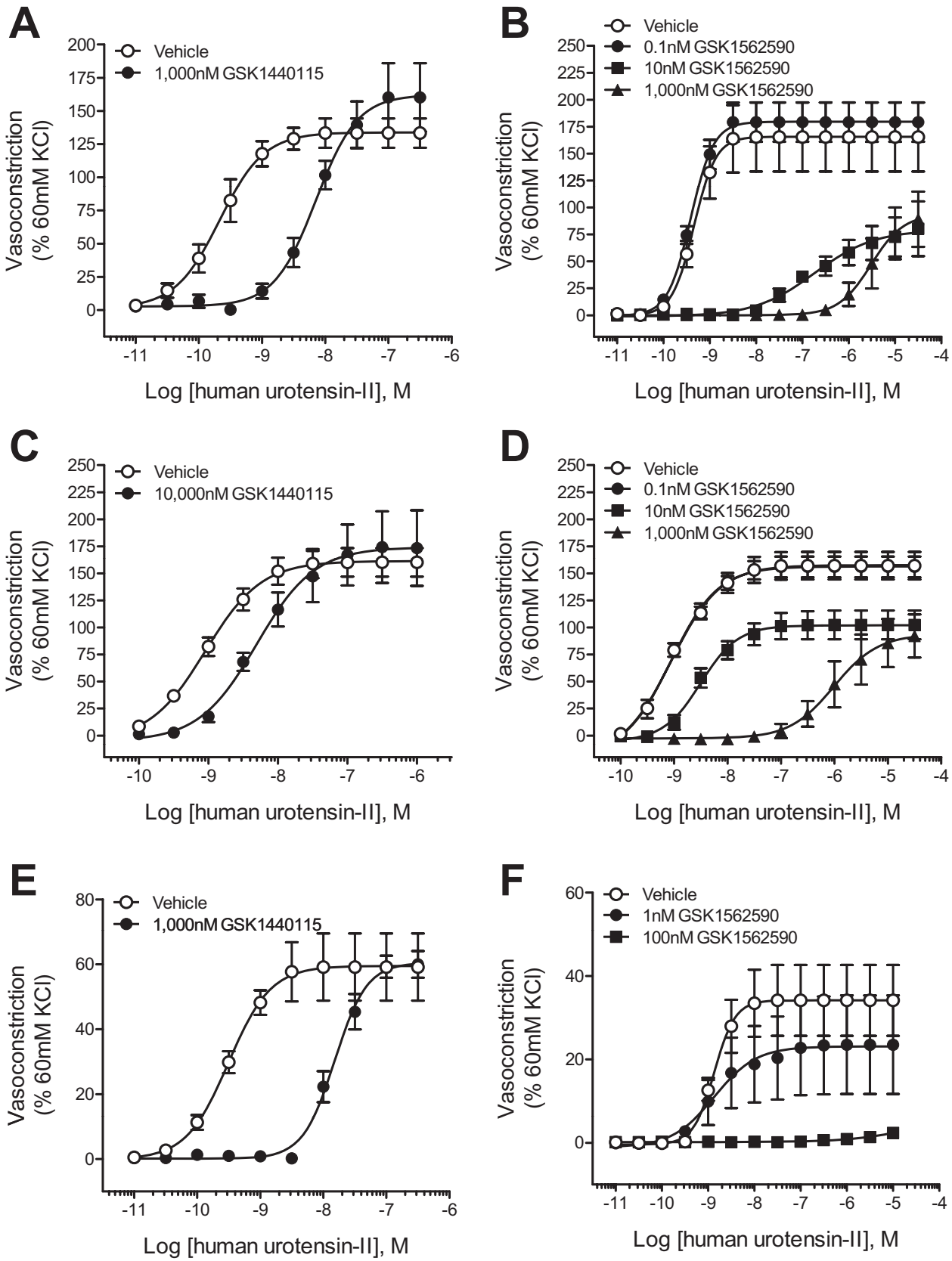
A
Vehicle
1,000nM GSK1440115
Vasoconstriction (% 60mM KCl)
Log [human urotensin-II], M
B
Vehicle
0.1nM GSK1562590
10nM GSK1562590
1,000nM GSK1562590
Vasoconstriction (% 60mM KCl)
Log [human urotensin-II], M
C
Vehicle
10,000nM GSK1440115
Vasoconstriction (% 60mM KCl)
Log [human urotensin-II], M
D
Vehicle
0.1nM GSK1562590
10nM GSK1562590
1,000nM GSK1562590
Vasoconstriction (% 60mM KCl)
Log [human urotensin-II], M
E
Vehicle
1,000nM GSK1440115
Vasoconstriction (% 60mM KCl)
Log [human urotensin-II], M
F
Vehicle
1nM GSK1562590
100nM GSK1562590
Vasoconstriction (% 60mM KCl)
Log [human urotensin-II], M

Figure 3

Inhibitory effects of GSK1440115 and GSK1562590 on hU-II-induced contraction of cat isolated arteries. GSK1440115 competitively inhibited (no suppression of the hU-II maximum contractile response) contractions elicited with hU-II in cat isolated (A) thoracic aortae (C) femoral arteries and (E) mesenteric resistance arteries. In contrast to GSK1440115 and consistent with its effects in rat isolated arteries, GSK1562590 suppressed the maximal response to hU-II in cat isolated (B) thoracic aortae (D) femoral arteries and (F) mesenteric resistance arteries.

Table 5

Inhibition of hU-II-induced contraction of isolated arteries from cat, monkey and human UT transgenic mouse by GSK1440115

	[GSK1440115] nM	hU-II E_{max} (% KCl) Vehicle-treated control	GSK1440115-treated	hU-II pEC_{50} Vehicle-treated control	GSK1440115-treated	pA_2
Cat						
Femoral artery (n = 5)	1 000	134 ± 11	161 ± 26	9.69 ± 0.15	8.28 ± 0.15	7.39 ± 0.16
Thoracic aorta (n = 5)	10 000	161 ± 13	173 ± 34	9.03 ± 0.08	8.33 ± 0.07	5.59 ± 0.12
Mesenteric resistance artery (n = 3)	1 000	59 ± 10	60 ± 4	9.56 ± 0.18	7.84 ± 0.13	7.71 ± 0.06
Monkey						
Renal artery (n = 4)	10 000	133 ± 34	109 ± 14	9.46 ± 0.08	7.82 ± 0.12	6.63 ± 0.16
Superior mesenteric artery (n = 4)	10 000	178 ± 19	158 ± 37	9.27 ± 0.16	7.80 ± 0.23	6.46 ± 0.09
Human UT transgenic mouse						
Thoracic aorta (n = 5)	10 000	128 ± 7	158 ± 16	9.15 ± 0.06	6.73 ± 0.07	7.41 ± 0.06

All values are expressed as mean ± SEM. Statistical comparisons of E_{max} values were performed using paired, two-tailed t-tests and no values were determined different from vehicle control values ($P > 0.05$). Competitive antagonist affinities (pA_2) were determined using the Schild equation (Jenkinson *et al.*, 1998).

hU-II-induced contraction (Figure 5B, Table 6). The estimated inhibitor potency (pA_2) was >8.5, making GSK1562590 at least an order of magnitude more potent than GSK1440115 in this vascular tissue.

Selective inhibition of hU-II contraction in rat isolated aorta

GSK1440115 (3 μM) did not attenuate the contractile actions of endothelin-1, phenylephrine or KCl on the rat isolated aorta ($pA_2 < 5.5$; Table 7). Similarly, at a concentration of 300 nM [>3 orders of magnitude over the hU-II pK_b in this tissue (10.21)], GSK1562590 failed to alter contraction elicited by endothelin-1, phenylephrine or KCl (Table 8). As such, both GSK1440115 and GSK1562590 are selective at inhibiting the contractile actions of hU-II in this preparation.

Reversibility of UT antagonism by washout in rat isolated aorta: in vitro *studies*

Exposure of rat isolated aortae to 0.3 μM GSK1440115 (with no washing) produced a parallel rightward-shift in the hU-II concentration–response curve with an EC_{50} ratio of 18.9, as expected for a competitive antagonist. The extent of hU-II inhibition was significantly reduced, however, when pretreatment with GSK1440115 was immediately followed by extensive (90 min) washing prior to construction of hU-II concentration–response curves. Under these conditions, a dose ratio of 3.0 was obtained *i.e.* antagonism with 0.3 μM GSK1440115 was attenuated 84% by washing (Figure 6A,B). This result is consistent with a reversible mode of UT occupancy.

In contrast to GSK1440115, repeatedly rinsing the tissue with fresh Krebs solution for 2 h to ≤16 h failed to reverse the inhibitory effects of 0.3 nM GSK1562590 *in vitro* (Figure 6C,D).

Reversibility of UT antagonism in rat isolated aorta: ex vivo *studies*

As significant GSK1562590 reversibility was not evident within the time constraints of the standard *in vitro* assay (tissue viability is an issue at ≥16 h), *ex vivo* studies were performed. In initial studies,

Table 6

Inhibitory effects of GSK1562590 on hU-II-induced contraction of cat and human UT transgenic mouse isolated arteries

	[GSK1562590] nM	hU-II E_{max} (% KCl) Vehicle-treated control	hU-II E_{max} (% KCl) GSK1562590-treated	hU-II pEC_{50} Vehicle-treated control	hU-II pEC_{50} GSK1562590-treated	pK_b
Cat						
Femoral artery (n = 3–4)	0.1	166 ± 32	180 ± 18	9.36 ± 0.05	9.44 ± 0.04	–
	10	148 ± 38	81 ± 27	9.36 ± 0.07	6.84 ± 0.31	10.12 ± 0.27
	1000	166 ± 32	93 ± 26	9.36 ± 0.05	5.45 ± 0.17	9.88 ± 0.29
Thoracic aorta (n = 4)	0.1	157 ± 13	156 ± 10	8.94 ± 0.08	8.95 ± 0.07	–
	10	157 ± 13	102 ± 13**	8.94 ± 0.08	8.44 ± 0.06	8.93 ± 0.23
	1000	157 ± 13	93 ± 19**	8.94 ± 0.08	5.88 ± 0.19	9.09 ± 0.28
Mesenteric resistance artery (n = 4)	1	34 ± 8	23 ± 12	8.89 ± 0.05	8.75 ± 0.19	–
	100	34 ± 8	0*	8.89 ± 0.05	-[ND]	>7.0
Human UT transgenic mouse						
Thoracic aorta (n = 5)	3	68±5	0***	8.81±0.08	-[ND]	>8.5

All values are expressed as mean ± SEM. Statistical comparisons of E_{max} values were performed using paired, two-tailed t-tests or ANOVA analysis with a Dunnett's post-test where *P < 0.05, **P < 0.01 and ***P < 0.001 versus vehicle control values. Noncompetitive antagonist affinities (pK_b) were determined using the method of Gaddum where equiactive concentrations of agonist in the absence or presence of the noncompetitive antagonist were compared in a linear regression (Gaddum *et al.*, 1955; Kenakin, 2006).

Figure 4

Competitive inhibition of hU-II-induced contraction of monkey isolated arteries by GSK1440115 and GSK1562590. GSK1440115 (10 000 nM) antagonized hU-II-induced contractions in monkey isolated (A) renal and (C) superior mesenteric arteries without suppressing the maximal contractile response. Similarly, GSK1562590 elicited parallel, rightward shifts to the hU-II concentration–response curve in both (B) renal and (D) superior mesenteric arteries, consistent with competitive hU-II antagonism. Clark plot analysis (global nonlinear regression) of GSK1562590 in (E) renal and (F) superior mesenteric arteries revealed pA_2 values of 8.93 (8.47–9.39 95% CI) and 8.87 (8.32–9.43 95% CI) and slopes of 0.89 (0.73–1.05 95% CI) and 0.96 (0.75–1.17 95% CI), respectively, consistent with a competitive mode of antagonism.

rat aortae were isolated 2 h (predetermined T_{max}) following oral dosing with 0.01–100 mg·kg^{-1} GSK1562590. Doses of ≥1 mg·kg^{-1} significantly inhibited hU-II contraction in isolated aortae assessed *ex vivo* (e.g. 66% inhibition at 1 mg·kg^{-1} GSK1562590, *p.o.*; Figure 7A).

In a follow-on temporal study, the maximal contractile responses to hU-II were significantly attenuated *ex vivo* for up to 36 h after dosing at 1 mg·kg^{-1} GSK1562590, *p.o.* (Figure 7B–C; Table 9). However, no hU-II inhibition was observed in vessels harvested 36–48 h following oral administration of 1 mg·kg^{-1} GSK1562590 (Figure 7D–E; Table 9).

At 1 mg·kg^{-1} *p.o.*, plasma levels of ~1 nM were attained at 2 h (approximately 10-fold over the K_b in the rat isolated aorta). Interestingly, GSK1562590 plasma levels were extremely low or undetectable at ≥16 h (<70 pM [lowest limit of quantification]; Figure 7E; Table 9). As such, plasma exposure underestimates the pharmacodynamic duration of action of GSK1562590, consistent with a slow k_{off} of GSK1562590 from rat UT. The inhibition was selective for hU-II as neither KCl nor phenylephrine contraction was altered at any time point studied (data not shown). Although GSK1440115 was not profiled under these conditions, an alternative non-pyrrolidine (*i.e.* morpholino) analog, GSK1575988, which functioned as a competitive, reversible UT antagonist in rat isolated aorta, was profiled under these *ex vivo* conditions and caused minimal (*i.e.* insignificant) inhibition at T_{2h} (data not shown).

Reversibility of GSK1562590 binding to rat, monkey and human UT

To verify that the slow *in vitro* and *ex vivo* 'washout' from rat tissues directly correlated with a slow dissociation of GSK1562590 from the rat UT, radioligand binding reversibility studies were performed using recombinant rat, monkey and human UT.

Compared with treatment with vehicle, 10 nM GSK1562590 attenuated the observed B_{max} for [^{125}I]hU-II binding by 5.2–38.3% (Table 10),

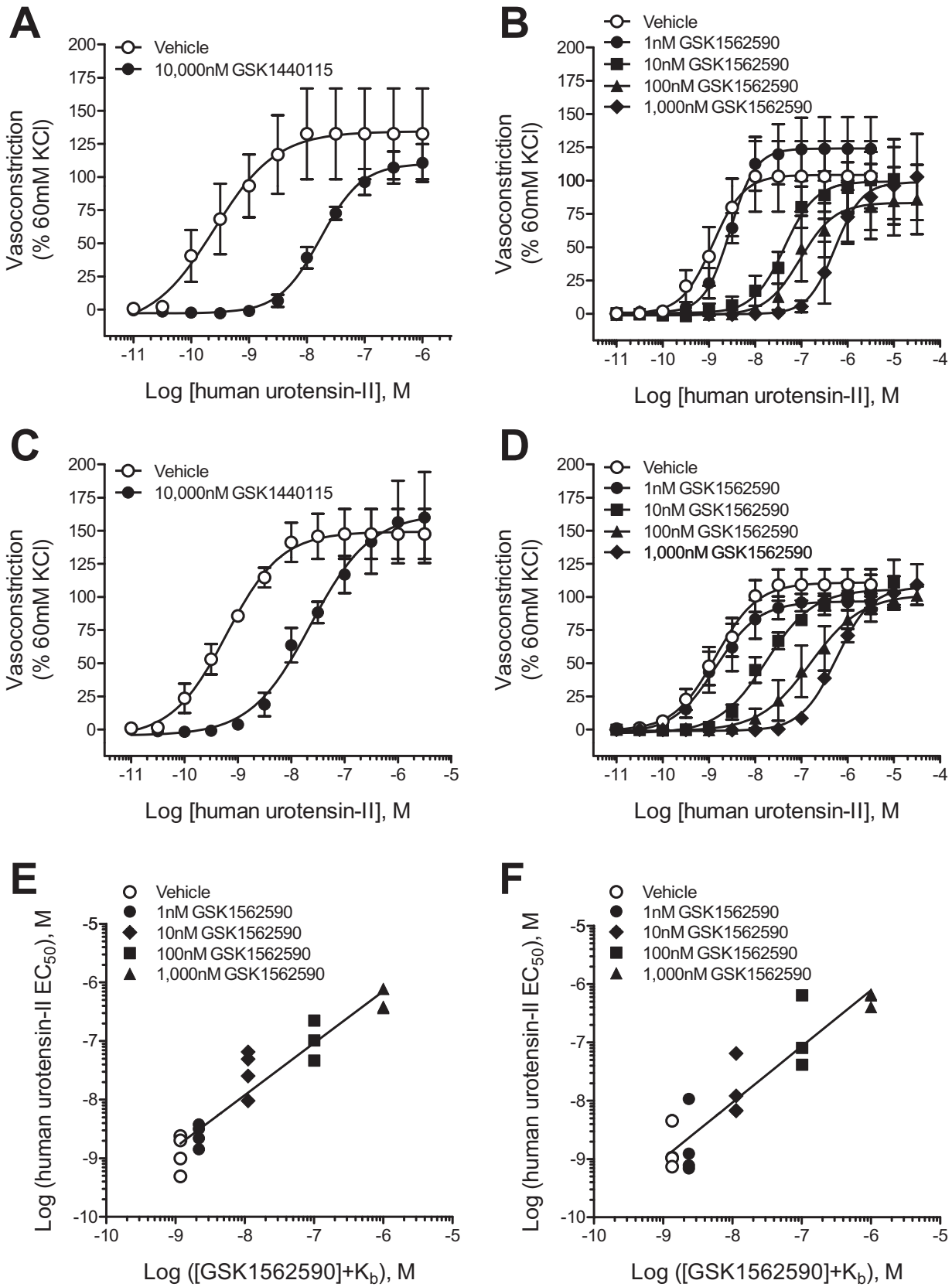
A
Vehicle
10,000nM GSK1440115
Vasoconstriction (% 60mM KCl)
Log [human urotensin-II], M
B
Vehicle
1nM GSK1562590
10nM GSK1562590
100nM GSK1562590
1,000nM GSK1562590
Vasoconstriction (% 60mM KCl)
Log [human urotensin-II], M
C
Vehicle
10,000nM GSK1440115
Vasoconstriction (% 60mM KCl)
Log [human urotensin-II], M
D
Vehicle
1nM GSK1562590
10nM GSK1562590
100nM GSK1562590
1,000nM GSK1562590
Vasoconstriction (% 60mM KCl)
Log [human urotensin-II], M
E
Vehicle
1nM GSK1562590
10nM GSK1562590
100nM GSK1562590
1,000nM GSK1562590
Log (human urotensin-II EC50), M
Log ([GSK1562590]+Kb), M
F
Vehicle
1nM GSK1562590
10nM GSK1562590
100nM GSK1562590
1,000nM GSK1562590
Log (human urotensin-II EC50), M
Log ([GSK1562590]+Kb), M

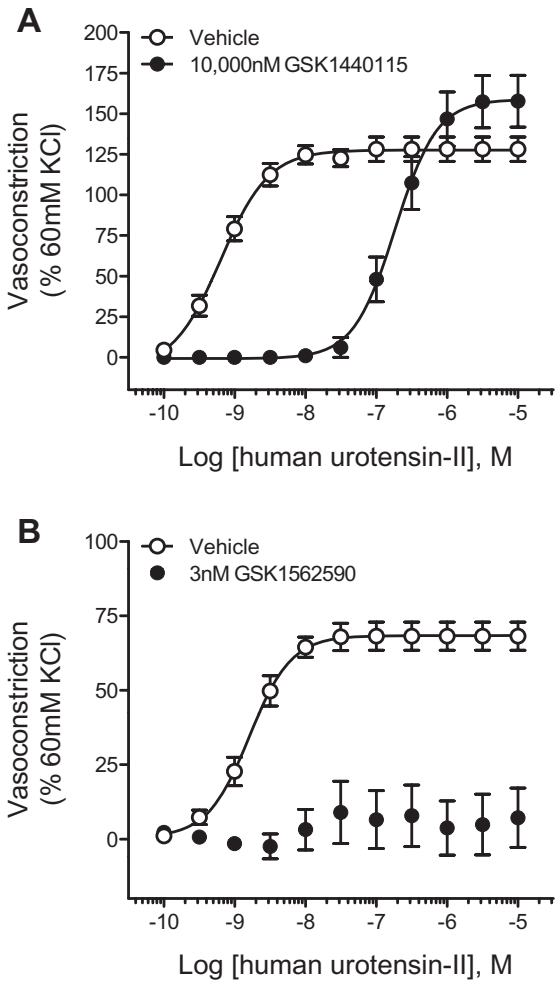

Figure 5

Inhibition of hU-II-induced contraction of isolated aortae from hUT transgenic mice by (A) GSK1440115 and (B) GSK1562590. Whereas pretreatment with 10 000 nM GSK1440115 elicited a parallel, rightward shift in the hU-II concentration–response curve (consistent with competitive hU-II antagonism), 3 nM GSK1562590 abolished the contractile responses to hU-II.

7.6–10.2% and 11.9% (data not shown) at washout t = 0, 0.5 and 1 h, respectively, for cell membranes expressing recombinant rat UT (n = 2). In contrast, GSK1562590 binding to membranes enriched with recombinant monkey receptor was fully reversible, exhibiting B_{max} values of 92.5 ± 5.2% (Table 10) and 94.2 ± 5.6% (data not shown) at washout t = 0 and 2 h, respectively, compared with vehicle-treated membranes (n = 4). Binding of GSK1562590 (10 nM) to membranes containing recombinant human UT was also reversible, but slower than that observed for the monkey receptor, exhibiting a B_{max} of 38.5–61.2% of vehicle-treated membranes immediately after washing (t = 0; n = 2; Table 10). GSK1562590 (10 nM) did not significantly alter the K_D values for [^{125}I]hU-II for any of the three UT orthologues studied (data not shown).

In vivo *cat hemodynamics*

GSK1440115 did not alter basal hemodynamics or ECG parameters in the anaesthetized cat at concentrations ≤3 mg·kg^{-1}. In contrast, at the highest dose tested (10 mg·kg^{-1}), GSK1440115 reduced basal arterial blood pressure by ~20 mmHg when compared with vehicle-treated cats, an effect accompanied by reduced left ventricular systolic pressure and left ventricular relaxation (-dP/dt) and elevated QRS and ST segments (P < 0.05). GSK1440115 attenuated the *in vivo* pressor response to 1 nmol·kg^{-1} hU-II at a minimally active pharmacological dose of 1 mg·kg^{-1}. Surprisingly, significant inhibition of hU-II effects was also observed using 10 mg·kg^{-1} GSK1440115 but not at the intermediate dose of 3 mg·kg^{-1} (Figure 8A,C).

In contrast with GSK1440115, GSK1562590 (0.01–10 mg·kg^{-1}) did not alter any basal haemodynamic or ECG parameters at any dose studied. GSK1562590 blocked the pressor actions of hU-II at 0.1 mg·kg^{-1}, a 10-fold lower dose than that required for GSK1440115 (Figure 8B,D).

The plasma levels achieved following administration of both compounds were approximately dose linear (data not shown).

Discussion and conclusions

Delineation of the (patho)physiological role of the U-II system has been hampered by the absence of potent and selective UT antagonists. Indeed, the lack of efficacy observed with Palosuran (ACT-058362; Clozel *et al.*, 2004; 2006; http://www1.actelion.com/documents/publications/Milestones_Company.pdf) in patients with diabetic nephropathy (phase IIb) was clouded by its low antagonist potency in whole cells and tissues (Behm *et al.*, 2008). As such, drug discovery programmes continue to focus on identifying potent and selective UT antagonists suitable for assessment in both preclinical species and man. The present study describes two compounds, GSK1440115 and GSK1562590, which fit these criteria.

Initial radioligand binding characterization of GSK1440115 and GSK1562590 indicated that both compounds were selective, high-affinity, pan-species active UT ligands, with GSK1562590 exhibiting a 5- to 101-fold greater potency than GSK1440115 across species. Aside from their unique potencies, the compounds were differentiated by their functional effects in rat isolated aorta. GSK1440115 behaved as a traditional *competitive*

Table 7

Selective effects of GSK1440115 (3 μM) on vasoconstrictor-induced contraction of the rat isolated aorta

Spasmogen	E_{max} (% KCl) Vehicle-treated control	GSK1440115-treated	pEC_{50} Vehicle-treated control	GSK1440115-treated
KCl	108 ± 3	108 ± 2	1.84 ± 0.03	1.83 ± 0.03
Phenylephrine	130 ± 4	128 ± 4	8.10 ± 0.02	7.94 ± 0.09
Endothelin-1	138 ± 5	129 ± 3	8.89 ± 0.08	8.89 ± 0.10

All values are expressed as mean ± SEM ($n = 5$). Statistical comparisons of E_{max} and pEC_{50} values were performed using paired, two-tailed *t*-tests and no values were determined different from vehicle control values ($P > 0.05$).

Table 8

Selective effects of GSK1562590 (0.3 μM) on vasoconstrictor-induced contraction of the rat isolated aorta

Spasmogen	E_{max} (% KCl) Vehicle-treated control	GSK1562590-treated	pEC_{50} Vehicle-treated control	GSK1562590-treated
KCl	116 ± 2	117 ± 2	1.83 ± 0.03	1.98 ± 0.06
Phenylephrine	129 ± 5	132 ± 4	8.07 ± 0.14	8.18 ± 0.13
Endothelin-1	138 ± 1	139 ± 3	8.73 ± 0.02	8.96 ± 0.05

All values are expressed as mean ± SEM ($n = 4$). Statistical comparisons of E_{max} and pEC_{50} values were performed using paired, two-tailed *t*-tests and no values were determined different from vehicle control values ($P > 0.05$).

antagonist, causing rightward shifts of the hU-II contractile concentration–response curve. In contrast, GSK1562590 elicited *insurmountable* antagonism, by which the maximal contractile response to hU-II was suppressed in a concentration-dependent manner. As discussed further below, we feel that this property of GSK1562590 might contribute to its enhanced efficacy *ex vivo*.

We envision several possible causes for the insurmountable antagonism exhibited by GSK1562590 in the rat aorta. Based on experience with pharmacophores from other chemical series, we initially suspected that GSK1562590 might suppress the maximal response to hU-II in a non-selective manner, for instance by altering smooth muscle cell Ca^{2+} modulation. However, this was not the case as GSK1562590 failed to alter vasoconstriction elicited via non-UT-related spasmogens including KCl, phenylephrine and endothelin-1.

Second, the insurmountable effects of GSK1562590 could be the result of a slow UT dissociation rate or covalent bonding modification of the receptor. As no evidence for covalent bonding has been identified to date, the antagonist is not considered truly *insurmountable* (irreversible inhibition through covalent bonding; Furchgott, 1966). Rather, we feel that our data are most consistent with a slowly reversible binding of GSK1562590 to UT. The phenomenon of slowly reversible inhibition was originally observed by Rang (1966) and has subsequently been used to describe the kinetics of action of several 'non UT' G-protein-coupled receptor antagonists including the AT_1 antagonists candsartan (Fierens *et al.*, 1999) and telmisartan (Maillard *et al.*, 2002) and the histamine H_1 antagonist desloratidine (Anthes *et al.*, 2002). GSK1562590 now represents the first identified slowly reversible, small molecule UT antagonist.

Although the exact molecular interaction responsible for the reduced dissociation rate (k_{off}) of GSK1562590 has not been identified, a key binding interaction of many GPCRs (including UT) involves a salt-bridge between an amino side-chain carboxylate and the ligand (Ji *et al.*, 1998; Ishiguro, 2004; Grieco *et al.*, 2009). It is therefore reasonable to hypothesize that this interaction may be accentuated with GSK1562590 due to the presence of the more basic pyrrolidine residue compared with the less basic morpholine in GSK1440115. Indeed, comparison of numerous pairs of pyrrolidine/morpholine analogs having otherwise identical chemical structures has demonstrated that without exception, the pyrrolidine analogues are 10–1000-fold more potent than their morpholine counter-

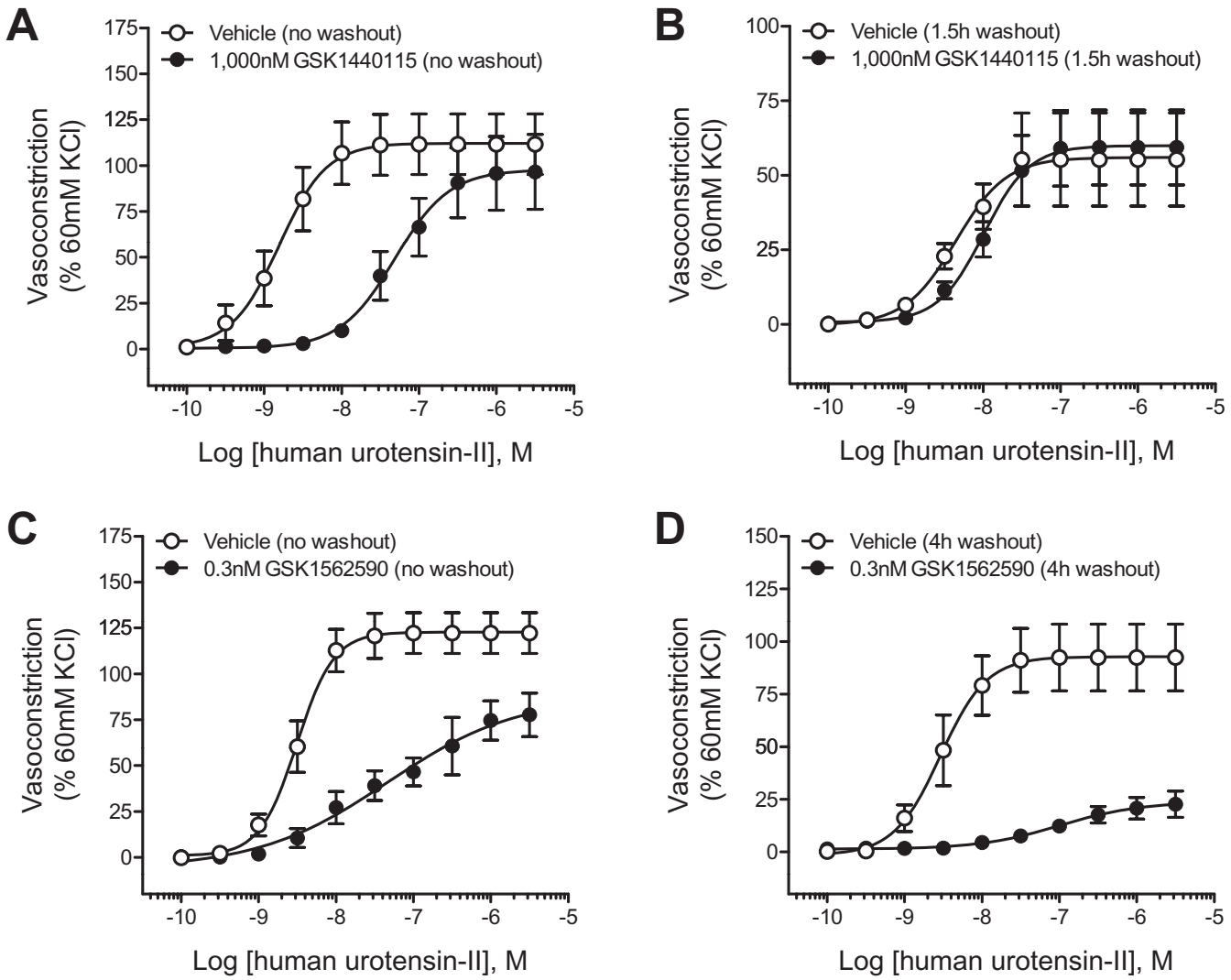

Figure 6

The inhibitory properties of (A, B) GSK1440115 but not (C, D) GSK1562590 were reversed by washout in the rat isolated aorta. Pre-incubation with 1000 nM GSK1440115 elicited parallel, rightward-shifts to the hU-II concentration–response curve (EC_{50} ratio of 18.9), and these inhibitory effects were reversible (EC_{50} ratio of 3.0) by repeatedly washing the tissues for 1.5 h with fresh Krebs solution (not containing antagonist) before generating the hU-II concentration–response curves. In contrast to GSK1440115, repeated rinsing of the tissue baths for 4 h failed to reverse the inhibitory effects of GSK1562590.

parts (McAtee *et al.*, 2008). In addition, a set of analogues in this chemical series with basic moieties other than pyrrolidine and morpholine exhibited a strong correlation between the basicity of the nitrogen functionality and UT binding affinity (data not shown).

Furthermore, the observation that GSK1562590 failed to cause a parallel shift of the hU-II concentration–response curve in the rat isolated aorta, at any concentration tested, is consistent with the rat aorta being devoid of spare receptors for U-II (Itoh *et al.*, 1987; Douglas *et al.*, 2004a). If spare receptors for U-II were present in this tissue, lower concentrations of GSK1562590, as an insurmountable antagonist, would be expected to elicit a parallel shift of the hU-II concentration–response curve and only when the number of receptors was reduced further by subsequent applications of GSK1562590 would there be an appreciable E_{max} reduction (Jenkinson, 1996). Our results therefore show that the nature of insurmountable antagonism observed in rat aorta likely reflects the combination of (a) a slow dissociation rate of GSK1562590 from rat UT and (b) a lack of spare receptors for U-II.

Overall, GSK1440115 appeared to function as a competitive UT antagonist in arteries from all species tested and the antagonism was fully surmountable by hU-II with a generally right-ward

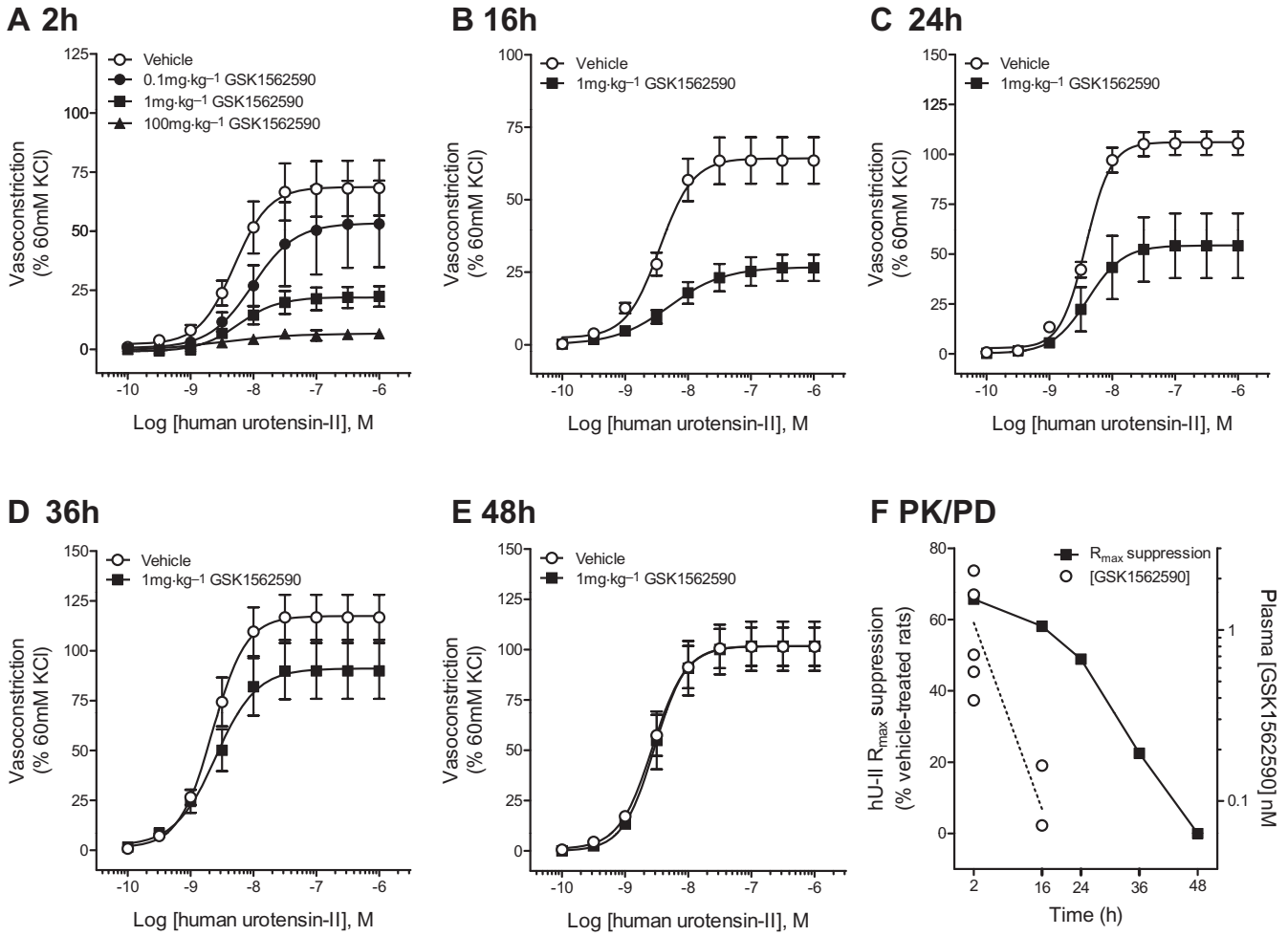

Figure 7

Inhibitory effects of GSK1562590 (1 mg·kg^{-1}, *p.o.*) on hU-II-induced contraction of rat aorta assessed *ex vivo*. (A) Rat aorta isolated 2 h (T_{max}) following oral dosing of GSK1562590 (0.1–100 mg·kg^{-1}) exhibited dose-dependent inhibition of hU-II contraction. The maximal contractile responses to hU-II were significantly inhibited by 1 mg·kg^{-1} GSK1562590 at (B) 16 h and (C) 24 h following oral dosing. No significant hU-II inhibition was observed in tissues harvested (D) 36 h and (E) 48 h following oral administration of 1 mg·kg^{-1} GSK1562590, consistent with a reversible mode of action. (F) Comparison of plasma drug levels and pharmacodynamic duration of action suggest a slow UT k_{off} for GSK1562590.

Table 9

Inhibitory effects of GSK1562590 (1 mg·kg^{-1}, *p.o.*) on hU-II-induced contraction of rat aorta *ex vivo*

Time (h)	Plasma concentration (nM)	hU-II pEC_{50}		hU-II E_{max} (% 60 mM KCl)	
		Vehicle	GSK1562590	Vehicle	GSK1562590
2	1.10 ± 0.35	8.35 ± 0.07	8.07 ± 0.18	66 ± 37	23 ± 9*
16	<0.12 ± 0.04†	8.52 ± 0.05	8.27 ± 0.09*	64 ± 8	27 ± 5*
24	<0.07	8.46 ± 0.02	8.29 ± 0.09	106 ± 6	54 ± 16*
36	<0.07	8.65 ± 0.05	8.61 ± 0.05	117 ± 11	91 ± 14
48	<0.07	8.56 ± 0.05	8.49 ± 0.07	102 ± 9	102 ± 12

All values are expressed as mean ± SEM (n = 5–7).

†Plasma concentrations below limit of detection (0.07 nM) for four out of six animals. Statistical comparisons of E_{max} and pEC_{50} values were made using unpaired, two-tailed *t*-tests where *P < 0.05 versus vehicle.

Table 10

Reversible interaction of GSK1562590 (10 nM) binding at rat, monkey and human recombinant UT

UT cell membrane	[^{125}I]hU-II B_{max} at washout t = 0 (% vehicle)	Time for [^{125}I]hU-II B_{max} >90% vehicle
Rat UT (n = 2)	5.2–38.3%	>1 h
Monkey UT (n = 4)	92.5 ± 5.2%	0 h
Human UT (n = 2)	38.5–61.2%	<1 h

All values are expressed as mean ± SEM, where n represents the number of individual experiments performed in duplicate. UT membranes were incubated with DMSO or 10 nM GSK1562590 for 30 min at 25°C following which the incubation mixtures were diluted, centrifuged and resuspended in buffer. Following resuspension, [^{125}I]hU-II K_D and B_{max} values were determined (t = 0). A subset of membranes were 'washed' a second time at various times following the initial resuspension (t = 0.5, 1 or 2 h) to assess GSK1562590 binding reversibility (time for [^{125}I]hU-II B_{max} >90% vehicle). K_D and B_{max} values were determined by homologous competition binding whereby multiple concentrations of unlabelled hU-II were used to compete for binding with a fixed concentration of [^{125}I]hU-II (Douglas *et al.*, 2005). GSK1562590 did not alter the K_D values for [^{125}I]hU-II for any of the three UT orthologues studied.

shift in agonist potency. However, in the absolute sense, GSK1440115 antagonism might depart from simple competitive binding interactions. For example, the highest concentration of GSK1440115 tested in the rat aorta (3 μM) caused no further shift to the hU-II concentration–response curve (*i.e.* Figure 2A). There are many potential explanations for deviation from pure competitive antagonism, such as reduced compound solubility at higher concentrations and differences in absolute mechanism between tissues, which we have yet to fully define for GSK1440115. In addition, antagonist potency was not consistent between tissues (e.g. Figure 3A,C,E). Indeed, concentrations of GSK1440115 ≤3 μM were not significantly inhibitory in the cat thoracic aorta (data not shown), and we caution that potencies might be underestimated in some tissues where only high concentrations of GSK1440115 (≥3 μM) elicited inhibitory effects. However, this phenomenon is not specific to GSK1440115, as other competitive UT antagonists also exhibit reduced potency in larger diameter arteries such as the cat thoracic aorta (Behm *et al.*, 2006; Behm *et al.*, 2008).

In contrast to the overall competitive nature of antagonism by GSK1440115 in arteries across species, the mode of antagonism observed with GSK1562590 was species-dependent with the compound functioning as an insurmountable UT antagonist in rat, cat and hUT transgenic mouse arteries but as a competitive antagonist in monkey arteries. Consistent with the functional data, the observed rank order of receptor dissociation rates for GSK1562590 from each receptor was: rat ≥ human > monkey UT. Thus, the insurmountable inhibitory effects of GSK1562590 likely reflect non-equilibrium conditions in rat, cat and hUT transgenic mouse arteries, where compound dissociation rates are much longer than the competing interaction. Unfortunately, additional studies aimed to further quantify receptor dissociation rates by increasing washout periods or temperature failed due to significant, time-dependent UT membrane degradation.

Tissue-based *in vitro* and *ex vivo* 'washout' studies provided further support for an extended duration of action for GSK1562590. Consistent with a competitive mode of antagonism, the inhibitory properties of GSK1440115 in the rat isolated aorta were readily reversed following a 1.5 h washout period. In contrast, no significant GSK1562590 reversibility was evident within the time of this standard *in vitro* washout assay (≤16 h). In follow-on *ex vivo* studies where rat aortae were isolated following oral dosing with GSK1562590, hU-II contraction was significantly inhibited in tissues from animals treated with GSK1562590 for up to 24 h. These results were surprising as plasma levels were undetectable at ≥16 h (<70 pM) and the tissues were suspended in Krebs buffer in the absence of any inhibitor for ~4 h before the hU-II concentration–response curves were generated. These data indicate that plasma exposure underestimates the pharmacodynamic duration of action of GSK1562590, consistent with extended UT residence time.

Consistent with the *in vitro* data, the compounds were readily differentiated in the anaesthetized cat, where GSK1562590 blocked the pressor actions of hU-II at 0.1 mg·kg^{-1} (plasma levels ≤6 ng·mL^{-1}), a 10-fold lower dose than that required for GSK1440115 (1 mg·kg^{-1}, plasma levels of ≤63 ng·mL^{-1}). Also, in contrast to GSK1440115, GSK1562590 failed to elicit any baseline blood pressure or ECG disturbances at any dose studied. Based on these observations, GSK1562590 not only exhibits higher efficacy but also greater selectivity as compared with GSK1440115 in this model.

Strikingly, significant suppression of the maximal contractile response for hU-II in rat isolated aorta was observed with concentrations of GSK1562590 as low as 0.1 nM, making it > two orders of magnitude more potent than GSK1440115 in this tissue. In addition, as compared with GSK1440115, which generally exhibited a ~10-fold loss in functional activity, minimal differences in potency between binding and functional assays

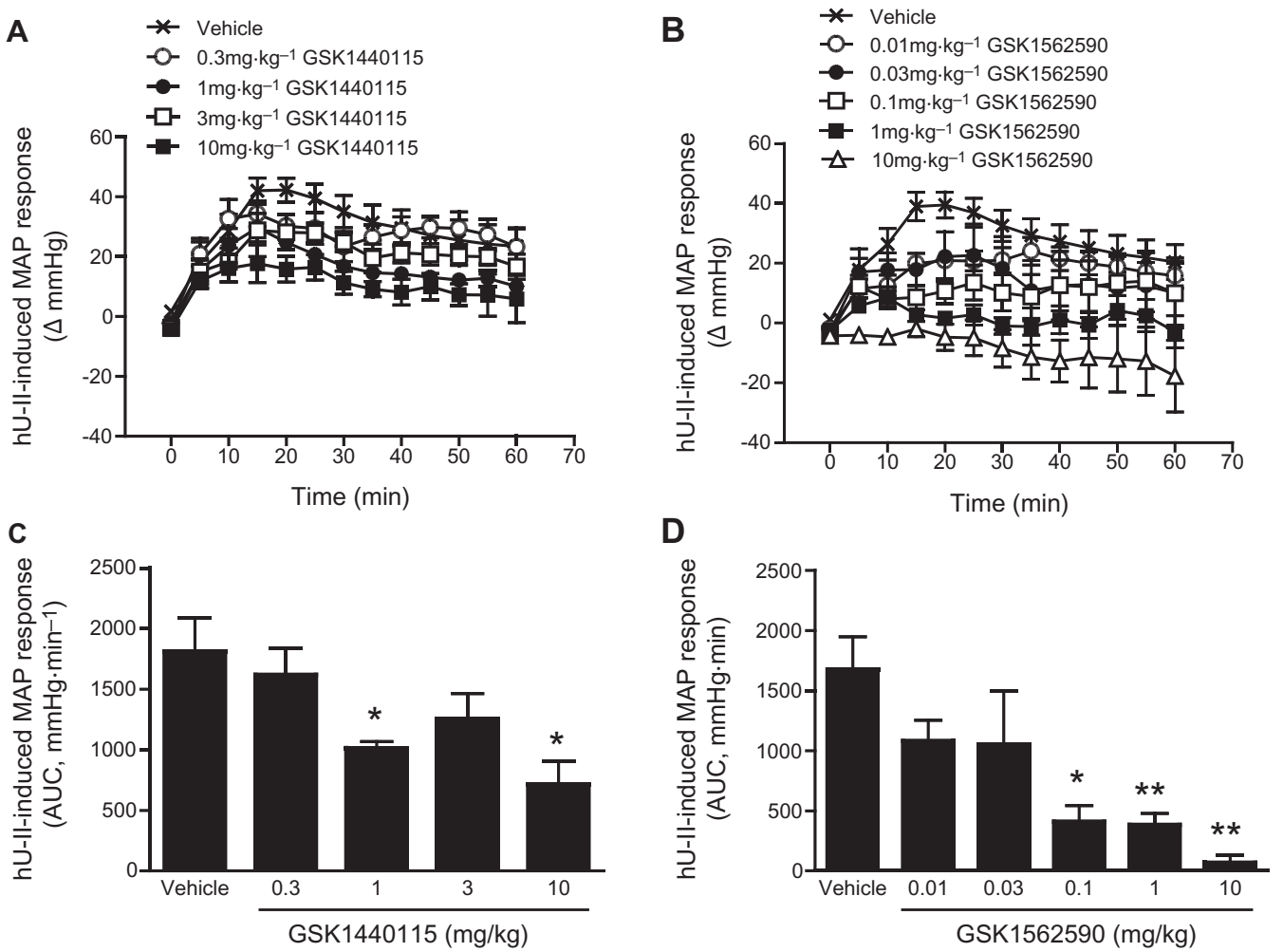

Figure 8

Inhibitory effects of GSK1440115 and GSK1562590 to exogenous hU-II challenge in the anaesthetized cat. The pressor response to hU-II (1 nmol·kg^{-1}, i.v. bolus) was dose-dependently inhibited by (A) GSK1440115 and (B) GSK1562590. Area under the mean arterial blood pressure responses for (C) GSK1440115 and (D) GSK1562590 indicated minimally active doses of 1 and 0.1 mg·kg^{-1} respectively.

was noted with GSK1562590. This constitutes a '*biochemical efficiency*', which is defined as the ratio of a compounds binding affinity (pK_i) to its functional response (pIC_{50}, pK_b, etc.) (Swinney, 2004), of approximately 0.1 and 1 for GSK1440115 and GSK1562590 respectively. Thus, as a consequence of an efficient non-equilibrium mechanism, GSK1562590 exhibits greater biochemical efficiency than GSK1440115, a characteristic that has been hypothesized to increase both the therapeutic window and efficacy of a drug (Swinney, 2004; Copeland *et al.*, 2006). Indeed, it is estimated that the percentage of marketed drugs with good biochemical efficiency (>0.4) is as high as 88% (Swinney, 2004). Interestingly, palosuran, which failed to show efficacy in diabetic nephropathy patients, exhibited a dramatic loss in UT potency in tissues, equivalent to biochemical efficiencies ranging from 0.1 to as low as 0.001 (Behm *et al.*, 2008).

Drugs with extended residence times (slow dissociation rates) have been linked to a beneficial extended duration of action *in vivo*. For example, the extremely slow dissociation rates of tiotropium versus ipratropium from the muscarinic (M_3) receptor and candesartan versus losartan from the AT_1 receptor are thought to contribute to their sustained and improved clinical actions (Laciurciére and Asmar, 1999; Van Noord *et al.*, 2002). Indeed, it has been recently proposed that compounds with this characteristic represent 'ultimate physiological inhibitors', where reversal of inhibition is dependent solely on target recycling by the organism (Copeland *et al.*, 2006). In addition, one can

hypothesize that a slow receptor off-rate might be even more important for UT antagonists to counteract the (a) pseudo-irreversible binding characteristics of U-II (Ames *et al*., 1999) and (b) the high levels of circulating 'U-II-like' immunoreactivity (~3 nM, ~2 orders of magnitude above the human UT K_d; Heller *et al*., 2002). We now add GSK1562590 to this list of ligands with extended residency.

In summary, both GSK1440115 and GSK1562590 represent high-affinity/selective UT antagonists suitable for interrogating the (patho)physiological role of the U-II system. In contrast to GSK1440115 which functions as a standard, rapidly reversible, competitive antagonist, GSK1562590 represents the first UT antagonist identified with enhanced UT residence time, resulting in extended duration of pharmacodynamic activity *ex vivo*. As compounds with enhanced residence time have been linked to improved therapeutic windows and increased efficacy, GSK1562590 constitutes an optimized tool for determining the (patho)physiology of the U-II pathway.

Acknowledgements

This paper is dedicated to the memory of our friend and colleague, Dr Stephen A. Douglas. The authors wish to thank D. Zhang and P.M. Eidam for compound scale-up, the MP CEDD DMPK group (specifically H.E. Fries and C.A. Evans) for bioanalytical support, Systems Research (specifically Z. Wu, L.H. Carballo, A.H. Ayscue, M.S. Jiang, E. Bettini and B. Oliosi) for technical assistance in assessing compound selectivity and C.P.A. Doe and G.P. Stankus for performing the cat exogenous U-II challenge model. We also thank Drs D.P. Brooks, J.G. Gleason and E.H. Ohlstein for meaningful discussion and insightful comments.

Conflict of interest

DJB, ARO, HEF, JJM, MAH, JWD, SED, GZW, KBG, CAS, MRH, RNW, MJN and CAL are current employees of GlaxoSmithKline.

References

Alexander SPH, Mathie A, Peters JA (2009). Guide to Receptors and Channels (GRAC), 4th edn. Br J Pharmacol 158 (Suppl. 1): S1–S254.

Ames RS, Sarau HM, Chambers JK, Willette RN, Aiyar NV, Romanic AM *et al*. (1999). Human urotensin-II is a potent vasoconstrictor and agonist for the orphan receptor GPR14. Nature 401: 282–286.

Anthes JC, Gilchrest H, Richard C, Eckel S, Hesk D, West RE *et al*. (2002). Biochemical characterization of desloratadine, a potent antagonist of the human histamine H_1 receptor. Eur J Pharmacol 449: 229–237.

Behm DJ, Doe CP, Johns DG, Maniscalco K, Stankus GP, Wibberley A *et al*. (2004). Urotensin-II: a novel systemic hypertensive factor in the cat. Naunyn Schmiedebergs Arch Pharmacol 369: 274–280.

Behm DJ, Stankus G, Doe CP, Willette RN, Sarau HM, Foley JJ *et al*. (2006). The peptidic urotensin-II receptor ligand GSK248451 possesses less intrinsic activity than the low-efficacy partial agonists SB-710411 and urantide in native mammalian tissues and recombinant cell systems. Br J Pharmacol 148: 173–190.

Behm DJ, McAtee JJ, Dodson JW, Neeb MJ, Fries HE, Evans CA *et al*. (2008). Palosuran inhibits binding to primate UT receptors in cell membranes but demonstrates differential activity in intact cells and vascular tissues. Br J Pharmacol 155: 374–386.

Cheng YC, Prusoff WH (1973). Relationship between the inhibition constant (Ki) and the concentration of inhibitor which causes 50 percent inhibition (IC_{50}) of an enzymatic reaction. Biochem Pharmacol 22: 357–366.

Clozel M, Binkert C, Birker-Robaczewska M, Boukhadra C, Ding SS, Fischli W *et al*. (2004). Pharmacology of the urotensin-II receptor antagonist palosuran (ACT-058362; 1-[2-(4-benzyl-4-hydroxy-piperidin-1-yl)-ethyl]-3-(2-methyl-quinolin-4-yl)-urea sulfate salt): first demonstration of a pathophysiological role of the urotensin system. J Pharmacol Exp Ther 311: 204–212.

Clozel M, Hess P, Qiu C, Ding SS, Rey M (2006). The urotensin-II receptor antagonist palosuran improves pancreatic and renal function in diabetic rats. J Pharmacol Exp Ther 316: 1115–1121.

Copeland RA, Pompliano DL, Meek TD (2006). Drug-target residence time and its implication for lead optimization. Nat Rev Drug Discov 5: 730–739.

Douglas SA, Sulpizio AC, Piercy V, Sarau HM, Ames RS, Aiyar NV *et al*. (2000). Differential vasoconstrictor activity of human urotensin-II in vascular tissue isolated from the rat, mouse, dog, pig, marmoset and cynomolgus monkey. Br J Pharmacol 131: 1262–1274.

Douglas SA, Dhanak D, Johns DG (2004a). From 'gills to pills': urotensin-II as a regulator of mammalian cardiorenal function. Trends Pharmacol Sci 25: 76–85.

Douglas SA, Naselsky D, Ao Z, Disa J, Herold CL, Lynch F *et al*. (2004b). Identification and pharmacological characterization of native, functional human urotensin-II receptors in rhabdomyosarcoma cell lines. Br J Pharmacol 142: 921–932.

Douglas SA, Behm DJ, Aiyar NV, Naselsky D, Disa J, Brooks DP *et al*. (2005). Non-peptidic Urotensin-II Receptor (UT) Antagonists I: *in vitro* pharmacological characterisation of SB-706375. Br J Pharmacol 145: 620–635.

Fierens FL, Vanderheyden PM, De Backer JP, Vauquelin G (1999). Insurmountable angiotensin AT1 receptor antagonists: the role of tight antagonist binding. Eur J Pharmacol 372: 199–206.

Furchgott RF (1966). The use of β-haloalkylamines in the differentiation of receptors and in the determination of dissociation constants of receptor-agonist complexes. Adv Drug Res 3: 21–55.

Gaddum JH, Hameed KA, Hathway DE, Stephens FF (1955). Quantitative studies of antagonists for 5-hydroxytryptamine. Q J Exp Physiol 40: 49–74.

Gong H, Wang YX, Zhu YZ, Wang WW, Wang MJ, Yao T *et al*. (2004). Cellular distribution of GPR14 and the positive inotropic role of urotensin II in the myocardium in adult rat. J Appl Physiol 97: 2228–2235.

Grieco P, Carotenuto A, Campiglia P, Gomez-Monterrey I, Auriemma L, Sala M *et al*. (2009). New insight into the binding mode of peptide ligands at Urotensin-II receptor: structure-activity relationships study on P5U and urantide. J Med Chem 52: 3927–3940.

Heller J, Schepke M, Neef M, Woitas R, Rabe C, Sauerbruch T (2002). Increased urotensin II plasma levels in patients with cirrhosis and portal hypertension. J Hepatol 37: 767–772.

Ishiguro M (2004). Ligand-binding modes in cationic biogenic amine receptors. Chembiochem 5: 1210–1219.

Itoh H, Itoh Y, Rivier J, Lederis K (1987). Contraction of major artery segments of rat by fish neuropeptide urotensin II. Am J Physiol Regul Integr Comp Physiol 252: R361–R366.

Jenkinson DH (1996). Classical approaches to the study of drug-receptor interactions. In: Foreman JC, Johansen T (eds). Textbook of Receptor Pharmacology. CRC Press: Boca Raton, FL, pp. 47–49.

Jenkinson DH, Barnard EA, Hoyer D, Humphrey PPA, Leff P, Shankley NP (1998). Terms and symbols in quantitative pharmacology. In: Girdlestone D (ed.). The IUPHAR Compendium of Receptor Characterization and Classification. IUPHAR Media: London, pp. 6–20.

Ji TH, Grossmann M, Ji I (1998). G protein-coupled receptors. I. Diversity of receptor-ligand interactions. J Biol Chem 273: 17299–17302.

Johns DG, Ao Z, Naselsky D, Herold CL, Maniscalco K, Sarov-Blat L *et al*. (2004). Urotensin-II-mediated cardiomyocyte hypertrophy: effect of receptor antagonism and role of inflammatory mediators. Naunyn Schmiedebergs Arch Pharmacol 370: 238–250.

Kenakin T (2006). Orthosteric drug antagonism. In: A Pharmacology Primer: Theory, Applications, and Methods. Academic Press: Massachusetts, pp. 114–119.

Laciurciére Y, Asmar RA (1999). A comparison of the efficacy and duration of action of candesartan cilexetil and losartan as assessed by clinic and ambulatory blood pressure after a missed dose in truly hypertensive patients. Am J Hypertens 12: 1181–1187.

Lew MJ, Angus JA (1997). An improved method for analysis of competitive agonist/antagonist interactions by non-linear regression. Ann NY Acad Sci 812: 179–181.

Liu JC, Chen CH, Chen JJ, Cheng TH (2009). Urotensin II induces rat cardiomyocyte hypertrophy via the transient oxidization of Src homology 2-containing tyrosine phosphatase and transactivation of epidermal growth factor receptor. Mol Pharmacol 76: 1186–1195.

McAtee JJ, Dodson JW, Dowdell SE, Erhard K, Girard GR, Goodman KB *et al*. (2008). Potent and selective small-molecule human urotensin-II antagonists with improved pharmacokinetic profiles. Bioorg Med Chem Lett 18: 3716–3719.

Maillard MP, Perregaux C, Centeno C, Stangier J, Wienen W, Brunner HR *et al*. (2002). *In vitro* and *in vivo* characterization of the activity of telmisartan: an insurmountable angiotensin II receptor antagonist. J Pharmacol Exp Ther 302: 1089–1095.

Maryanoff BE, Kinney WA (2010). Urotensin-II receptor modulators as potential drugs. J Med Chem 53: 2695–2708.

Onan D, Pipolo L, Yang E, Hannan RD, Thomas WG (2004). Urotensin II promotes hypertrophy of cardiac myocytes via mitogen-activated protein kinases. Mol Endocrinol 18: 2344–2354.

Quaile MP, Kubo H, Kimbrough CL, Douglas SA, Margulies KB (2009). Direct inotropic effects of exogenous and endogenous urotensin-II: divergent actions in failing and nonfailing human myocardium. Circ Heart Fail 2: 39–46.

Rang HP (1966). The kinetics of action of acetylcholine antagonists in smooth muscle. Proc R Soc Lond B Biol Sci 164: 488–510.

Russell FD, Molenaar P, O'Brien DM (2001). Cardiostimulant effects of urotensin-II in human heart in vitro. Br J Pharmacol 132: 5–9.

Sidharta PN, Wagner FD, Bohnemeier H, Jungnik A, Halabi A, Krawhenbuehl S *et al*. (2006). Pharmacodynamics and pharmacokinetics of the urotensin II receptor antagonist palosuran in macroalbuminuric, diabetic patients. Clin Pharmacol Ther 80: 246–256.

Sidharta PN, Van Giersbergen PLM, Dingemanse J (2009). Pharmacodynamics and pharmacokinetics of the urotensin II receptor antagonist palosuran in healthy male subjects. J Clin Pharmacol 49: 1168–1175.

Silvestre RA, Rodríguez-Gallardo J, Egido EM, Marco J (2001). Inhibition of insulin release by urotensin II – a study on the perfused rat pancreas. Horm Metab Res 33: 379–381.

Song W, Ashton N, Balment RJ (2003). Effects of single bolus urotensin II injection in anaesthetized rats. J Physiol 552P: P107.

Swinney DC (2004). Biochemical mechanisms of drug action: what does it take for success? Nat Rev Drug Discov 3: 801–808.

Tzanidis A, Hannan RD, Thomas WG, Onan D, Autelitano DJ, See F *et al*. (2003). Direct actions of urotensin II on the heart: implications for cardiac fibrosis and hypertrophy. Circ Res 93: 246–253.

Van Noord JA, Smeets JJ, Custers FLJ, Korducki L, Cornelissen PJG (2002). Pharmacodynamic steady state of tiotropium in patients with chronic obstructive pulmonary disease. Eur Respir J 19: 639–644.

Zhang AY, Chen YF, Zhang DX, Yi FX, Qi J, Andrade-Gordon P *et al*. (2003). Urotensin II is a nitric oxide-dependent vasodilator and natriuretic peptide in the rat kidney. Am J Physiol Renal Physiol 285: F792–F798.